Hinze, Cheryl L., Optimization of reconstituted high density lipoprotein nanoparticles as a delivery system for neuroblastoma treatment. Master of Science. (Biomedical Sciences), November 2013. 56pp., 2 tables, 29 illustrations, bibliography, 25 titles.

Despite many advances in cancer therapy over the last few decades, cancer remains one of the most common causes of death in not only the United States, but around the world. Two of the major problems cancer patients face today are the horrific side effects associated with chemotherapy, and the development of drug resistance. Both of these become even bigger problems when they are applied to children. Neuroblastoma is one of the most common forms of pediatric cancer. High risk Neuroblastoma patients are commonly faced with intensive multi-modal therapies in attempt to overcome a very aggressive disease. Due to the intensive therapy required, side effects can often linger even after remission is achieved in these patients, and multi-drug resistance is common due to the high levels of Doxorubicin administered. New solutions are needed in order to overcome both of these problems in Neuroblastoma as well as other types of cancer.

In this thesis, we studied the effects of different formulation and preparation techniques for the reconstituted high density lipoprotein nanoparticle model for anti-cancer agent delivery. During these studies we found that naturally derived mixes of phosphatidylcholine, and lower levels of apolipoprotein A-1 increase the encapsulation efficiency of the rHDL nanoparticles. We also determined that the addition of lyophilization during preparation before cholate dialysis, forms a more homogeneous preparation. After the optimization of the particle formulation and preparation, we tested the efficacy of two model anti-cancer agents in different cancer cells. First we showed the ability of the rHDL-siRNA nanoparticles to knockdown the SR-B1 protein is greater than the knockdown of a commercial transfection kit. Finally we prove that the rHDL

also improves the cytotoxic efficacy of a novel treatment for Neuroblastoma involving Imatinib Mesylate and Saquinavir.

In conclusion, the results of this thesis show a more detailed knowledge of the rHDL nanoparticle formulation as well as how it can be applied as an effective delivery system for both siRNA and chemotherapeutic agents. This data should help push our formulations closer to clinical applications, and toward helping reduce the toxic side effects of many chemotherapeutic agents, as well as reducing the incidence of drug resistance.

OPTIMIZATION OF RECONSTITUTED HIGH DENSITY LIPOPROTEIN NANOPARTICLES AS A DELIVERY SYSTEM FOR NEUROBLASTOMA TREATMENT

THESIS

Presented to the Graduate Council of the

Graduate School of Biomedical Sciences

University of North Texas

Health Science Center at Fort Worth

In Partial Fulfillment of the Requirements

For the Degree of

MASTER OF SCIENCE

By

Cheryl L. Hinze, B.A.

Fort Worth, Texas

November, 2013

ACKNOWLEDGEMENTS

First, I would like to thank my major professor, Dr. Andras G. Lacko for allowing me the opportunity to work in your laboratory and helping guide me through my research. Your advice and support throughout the progression of this research project was invaluable. Thank you so much.

I would also like to thank the members of my committee: Dr. Maya Nair, Dr. Eric B. Gonzales, and my university member, Dr. Abe Clark for their advice and support in helping me reach my research goals. Thank you for serving on my committee.

A very special thank you goes to my fellow lab members: Dr. Walter McConathy, Dr. Nirupama Sabnis, Becky Johnson, Dr. Anton Kosov, Bhavani and Ruben for all of their assistance in the lab. Dr. Nirupama Sabnis, thank you so much for all of your help, you taught me so much, and I could not have done any of this without you. Becky Johnson, thank you so much for keeping us all organized in lab, for teaching me everything there is to know about western blots, and for always making me laugh. Also I would like to thank the Berg lab: Aly and Mohana for always listening to my complaints and making me smile.

Finally, I would like to thank all of my family and friends who supported and encouraged me throughout my graduate career. To my parents, thank you so much for all of your love, support, and encouragement throughout not only graduate school, but my entire life, I would not be where I am today without you both. To my wonderful husband, thank you for putting up with the ups and downs of research with me, and for always listening, encouraging and supporting me to keep pushing forward.

TABLE OF CONTENTS

LIST OF TABLES

LIST OF FIGURES

CHAPTER I:

INTRODUCTION

Cancer is defined as an unregulated division and growth of cells, which often leads to the formation of solid masses referred to as tumors. Common treatment for cancer includes a combination of surgery, chemotherapy, and radiation therapy. Despite experimental advances in therapeutics, cancer remains the second most common cause of death in the United States according to the American Cancer Society. These findings are due to several factors, including metastasis, drug resistance and toxic side effects of most chemotherapeutic agents. Current cancer research is aimed at overcoming these and other factors, in part via the use of nanoparticles.

This research project was designed to optimize the formulation of a targeted delivery system for anti-cancer agents, aiming to increase the efficacy of known therapeutic agents against cancer cells and tumors. It is anticipated that the outcome of these studies will lead to improvements in the prospects for survival and the quality of life for cancer patients.

Background

Application of Nanoparticles for Cancer Therapy:

Nanoparticles have been studied for over two decades as delivery vehicles for siRNA and other anti-cancer agents in anticipation of the benefits accrued due their enhanced penetration into the tumor microenvironment. Nanoparticles thus have the capability to deliver their payload to a larger surface area of the tumor (than conventional chemotherapy approaches), leading to the

accelerated death of malignant cells. Many different types of nanoparticles have been developed to deliver chemotherapeutic drugs and siRNA. One of the most frequently employed types are in the group of lipid based nanoparticles, including liposomes [11], poly-lacto-co-glycolic acid (PLGA) nanoparticles, micelles, and gold nanoparticles [13]. The most widely used delivery vehicle formulations in cancer chemotherapy are liposomes due to their relatively easy preparation, highly stable formulations and their ability to be functionalized for tumor targeting. While liposomes represent effective drug delivery vehicles, the conjugation of targeting and stabilizing moieties such as polyethylene glycol (PEG) to the particle surface increases the diameter of the nanoparticles and may lead to induction of an undesirable immune response [14].

Reconstituted High Density Lipoproteins (rHDL)

Our laboratory has developed a novel drug delivery system consisting of reconstituted high density lipoproteins (rHDL) that transport anti-cancer agents selectively to cancer cells and tumors via the scavenger receptor type B1 (SR-B1). Circulating HDL is an important part of the reverse cholesterol transport pathway, facilitating the movement of excess peripheral cholesterol to the liver. The core components of the HDL complex (cholesteryl esters) can be accessed by tissues via the SR-B1 receptor. A previous study by our lab has shown that the SR-B1 receptor is overexpressed in most malignant cells [15]. We hypothesized that this overexpression is due to the need of malignant cells and tissues for excess amounts of cholesterol, to maintain their high proliferation rates [16]. The overexpression of the SR-B1 receptor allows for a “Trojan Horse” type delivery strategy where rHDL nanoparticles mimic normal circulating HDL, but are used to deliver anti-cancer agents to malignant cells and tumors instead of cholesterol [17].

Figure 1. Diagram of rHDL-siRNA nanoparticle

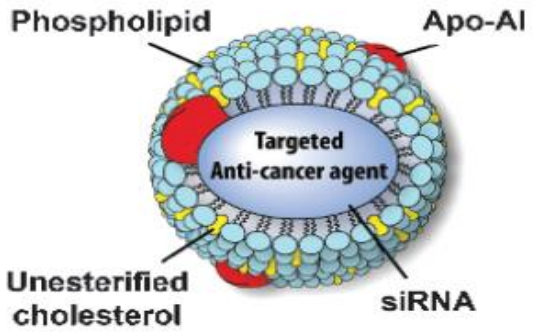

Advantages of rHDL as a Chemotherapeutic Delivery System:

Many chemotherapeutic agents are difficult to deliver systemically due to poor pharmacokinetics and bioavailability. For example, most chemotherapy drugs are poorly water soluble; however rHDL nanoparticles can solubilize these hydrophobic drugs by encapsulating them in a hydrophobic core and thus enhance their delivery to tumors [15]. Another concern is the unstable nature of siRNA which can be easily degraded by blood nucleases; rHDL can protect the siRNA by delivering it directly to the target cancer cells [12]. The rHDL system takes advantage of a two pronged delivery approach, via both passive as well as the active targeting to the SR-B1 receptor. The rHDL nanoparticles typically range from 10 nm to 20 nm in diameter, and therefore can take advantage of passive targeting through the leaky vasculature system of a tumor microenvironment (Figure 2). By directly targeting the malignant cells and tumors, our formulation should thus decrease the peripheral toxicities of the encapsulated chemotherapeutic agent, allowing for the possibility of using higher dosages, and achieve a better quality of life for the patient by reducing residual effects of the therapy.

Figure 2. Size comparison of liposomes to lipoproteins

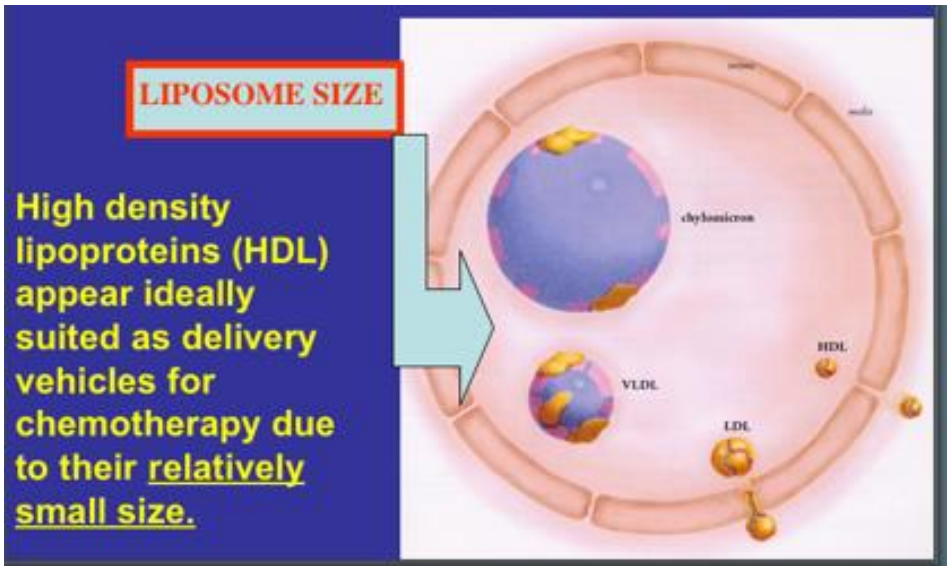

Neuroblastoma

Our laboratory has been focusing on neuroblastoma (NB) therapeutics because NB is an orphan disease and due to the opportunity for potentially rapid translation of the laboratory findings via collaboration with Cook Children's Medical Center (Fort Worth). NB is an embryonic cancer of sympaticoadrenal lineage [1]. It is the most common extra-cranial solid tumor diagnosed in children and the third most common form of pediatric cancer [2]. NB tumors have been known to develop within the sympathetic nervous system and are most commonly found in the abdominal region. NB has a very diverse clinical presentation with a wide range of corresponding prognoses. Tumors are classified based on neuroblast differentiation, Schwannian stroma content, mitosis-karyorrhexis index, MYCN gene amplification, dissemination and patient age. When diagnosed early and at a younger age (less than one year) the prognosis is usually very good requiring limited or no treatment to achieve remission. Late stage or high risk NB (HRNB), on the other hand, is very difficult to treat with a current survival rate of about forty percent. HRNB most often presents with a combination of all or some of the following

features: older age (18 months or older), tumor histology, amplification of the MYCN gene and dissemination to local bone, bone marrow or regional lymph nodes [1].

Current Therapy for Neuroblastoma

Current treatment for late stage or HRNB includes a combination of surgery to remove the primary tumor, and metastases when possible, followed by radiation and chemotherapy. Chemotherapy most commonly involves one of the following agents: doxorubicin, cisplatin, carboplatin, cyclophosphamide, vincristine, etoposide and topotecan [1]. Most of these drugs have severe off target toxicity (side effects), therefore their dosages must be limited while treating pediatric patients.

Problems with Current Neuroblastoma Therapy

The biggest problem with current pediatric cancer treatment, including NB, is the dose-limiting toxicities of the chemotherapeutic agents. All of the currently approved drugs for NB are also toxic to normal cells and tissues, which limits their clinical application because of numerous complications even subsequent to the completion of therapy. Recent studies with HRNB survivors indicate several residual impairments including: hearing loss, renal toxicity, and endocrine complications [3], specifically hypothyroidism that often requires thyroid replacement therapy and is associated with stunted growth, delayed puberty, and hypogonadism in males [4]. In addition, platinum containing drugs and cyclophosphamide have been linked to nephrotoxicity resulting in reduced glomerular filtration rate even among patients in remission. In a severe case, total loss of function in one kidney has been reported in conjunction with abdominal radiation therapy, and chemotherapy [4]. Due to these persisting problems, new drugs and

treatment methods are urgently needed to facilitate longer term survival rates, and to improve the quality of life during and subsequent to therapy.

An additional major problem with all types of cancer, including NB is drug resistance. There are two forms of drug resistance encountered with NB therapy: multi-drug resistance acquired by frequent treatment with doxorubicin (DOX), and environment mediated drug resistance (EMDR). The most common form of drug resistance is multi-drug resistance (MDR) characterized by the overexpression of ATP-cassette (ABC) transporter proteins on the cancer cell membranes [5, 9]. These transporters work as efflux pumps that eject the drugs out of the cancer cells, thus eliminating their cytotoxic effects [6]. On the other hand, EMDR functions by the up-regulation of survivin proteins by STAT3 and IL-6, thus protecting the cancer cells from drug induced apoptosis [7]. One way to attack both EMDR and MDR is through gene silencing therapy via either siRNA (small interfering RNA) knockdown or chemical inhibitors of either STAT3 or the ABC transporters [7, 8, 9].

The Emergence of Personalized Medicine in Cancer Therapy:

The general strategy for current cancer chemotherapy involves a “blanket approach”, where many of the same drugs or their combinations are used to treat most cases that involve the same type and stage of cancer. However, recent research has shown that each case of cancer may be unique with its own specific genetic makeup and tumor type, which suggests that there is a need for a more personalized/individualized approach to cancer treatment. Studies investigating future strategies for personalized medicine has advanced markedly in the past decade through the emergence of a massive amount of genomic and proteomic data. These current studies are aimed to identify suitable biomarkers for the identification of individual types of cancer, as well as

potential targets for therapy [23]. One specific example of a proteomics based application to personalized medicine is the identification of the protein pfetin as a prognostic biomarker for the metastatic potential in gastrointestinal stromal tumors [24]. Once this type of information becomes available for more types of cancer, personalized therapeutics may prove most effective for the treatment of each individual patient.

RNA Interference Therapy in Cancer:

One of the ways to take advantage of information provided by personalized genomic and/or proteomic data in cancer treatment is to directly target specific pathways involved with carcinogenesis and metastasis via RNA interference (RNAi) using small interfering RNA (siRNA). RNAi functions by degrading the messenger RNA (mRNA) for a specific protein via small interfering RNA (siRNA), before the mRNA can be translated into the protein or proteins that it specifically codes for. The loss of the functions of these key proteins is anticipated to limit or arrest the growth of the malignant cells and tumors or to induce apoptosis and thus preventing rapid tumor progression and metastasis. An additional benefit realized from gene targeting via siRNA could be an increased susceptibility of the cancer cells and tumors to chemotherapeutic agents thus opening the way for effective combination therapies. However, the clinical application of siRNA has been limited due to its size and highly anionic nature [10]. When delivered alone, blood nucleases degrade siRNA quickly within the bloodstream, and its fragments are subsequently cleared by the kidneys before it can reach the target cells [11, 12]. If any siRNA actually does reach the cells, it is often repelled due to the negative charges found on both the siRNA and on the surface of most cell membranes. Current RNAi research has been attempting to overcome these problems by encapsulating siRNA into different types of nanoparticles for delivery to *in vivo* targets.

Novel Drug Combination for Neuroblastoma Treatment:

Most of the currently used chemotherapeutic agents for NB are excessively hydrophilic for proper encapsulation into our system (rHDL nanoparticles) without modifications. However, in collaboration with Dr. Fabio Timeus from the University of Turin, Italy, our lab has been directed toward the study of a novel combination chemotherapy regimen for NB involving Imatinib Mesylate (Figure 3a) and Saquinavir (Figure 3b) [2]. Imatinib Mesylate (Imatinib) is a protein kinase inhibitor specific for c-kit (the receptor for stem cell factor (SCF)), platelet derived growth factor receptor (PDGFR), and Flk-1 (the receptor for vascular endothelial growth factor (VEGF)), all of which have a role in facilitating the progress of NB tumors [18]. Despite encouraging pre-clinical data, Imatinib has had limited clinical efficacy against NB tumors when used as a single agent [2]. Saquinavir is a protease inhibitor currently used in anti-HIV cocktail therapies. It has been noted that HIV patients taking protease inhibitors like Saquinavir, have a lower incidence of infection associated malignancies, therefore these inhibitors might have anti-cancer potential [12]. The anti-cancer activity of Saquinavir and other protease inhibitors has been studied *in vitro* for numerous malignancies including ovarian cancer [20], and leukemia [22]; it has been suggested that these agents work through a proteasome-independent blockage of angiogenesis [23]. Original studies completed by Dr. Timeus's lab in Italy show strong cytotoxic abilities for Imatinib, Saquinavir and several combinations of the two drugs [2]. Therefore we hypothesize that when both agents are encapsulated in rHDL, they may achieve superior therapeutic efficacy without the severe side effects normally associated with chemotherapy.

Figure 3a. Chemical Structure of Imatinib Mesylate

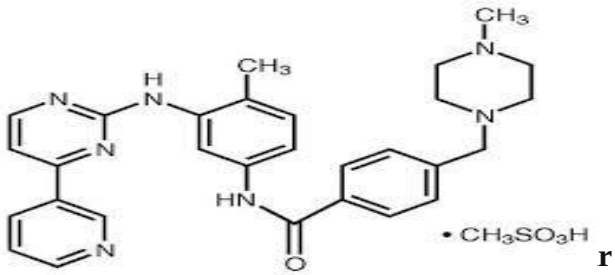

Figure 3b. Chemical Structure of Saquinavir

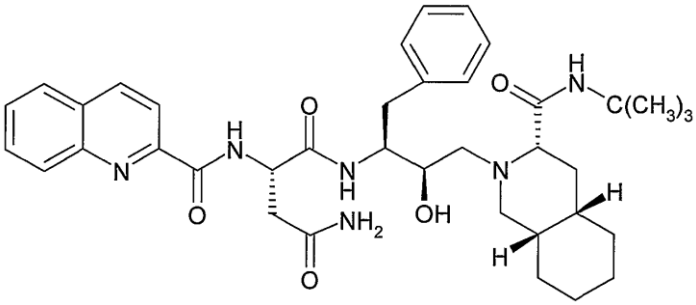

Objective:

The objective of this research project was to determine the optimal formulation for the preparation of drug containing rHDL nanoparticles for maximum efficacy against cancer cells, including NB cells. This objective was assessed by evaluating different compositions of the rHDL nanoparticles based on the efficiency of drug incorporation, size distribution and ratio of apolipoprotein to phospholipid content. Once the best formulations were determined, they were tested for *in vitro* cytotoxic efficacy and uptake by cancer cells.

Project Significance:

The optimization of this rHDL delivery system for formulations of both siRNA and chemotherapeutic drugs is anticipated to increase the encapsulation efficiency of the agents into the particles, and the uptake of the agents into the cancer cells and tumors, while decreasing the uptake of the agents by normal cells and tissues. An increase in drug uptake should increase the efficacy of the drug to kill the cancer cells, and therefore lower the dosages required during chemotherapy. Along with lower dosages, the protective core of the rHDL nanoparticles should lower the toxic side effects of the anti-cancer agents, allowing for improved prospects for survival and quality of life for cancer patients.

CHAPTER II

MATERIALS AND METHODS:

siRNA-rHDL Nanoparticle Preparation and siRNA Incorporation

STAT3 targeted siRNA and SR-B1 targeted siRNA (both gifts of Dr. Anil Sood, MD Anderson Cancer Center, Houston, TX) were used during these studies. The preparation of the siRNA containing rHDL nanoparticles followed the method of Shahzad et al [12]. Briefly, the lipid components including 3 µL of free cholesterol (FC), 3.5 µL cholesterol oleate (CE) (25 mg/mL stocks in chloroform), and 75 µL of egg-yolk phosphatidylcholine (100 mg/mL stock in chloroform) were mixed to form a molar ratio of 1:5:1.3:115, and then dried under a stream of nitrogen. For the alternate phospholipid component studies, 150 µL of soybean phosphatidylcholine or 1, 2 dioleoyl phosphatidylcholine (50 mg/mL stocks in chloroform) (Avanti Polar Lipids), were used. The siRNA (25 µg, 50 µg, or 100 µg from 100 µg/µL stock in DEPC treated deionized water) was boiled at 90°C for one minute and then incubated at 37°C for one hour. After incubation, the siRNA was combined with oligolysine (25mg/mL stock) at a 1:5 ratio (SIGMA; mean MW, 500-2000) at 37°C and then re-incubated for 30 minutes at 37°C. Apolipoprotein A-I (Apo A-I), was purchased from (MC LAB, San Francisco CA). The oligolysine/siRNA mixture was then combined with the dried lipids. Apo-A1 (7.24 mg/mL in PBS) was combined with the lipid mix at one of the following concentrations: 0.5 mg/mL, 1.0 mg/mL, 2.5 mg/mL or 4 mg/mL. Next, sodium cholate, 70 µl (100 mg/ml stock in 0.15 M NaCl, 0.003 M KCl, 0.15 M KH_2PO_4, pH 7.4 [designated as PBS]) was added to produce a final PC-to-

cholate molar ratio of ~1:1.6. The final volume was adjusted to 1 ml with buffer (10 mM Tris, 0.1 M KCl, 1 mM EDTA pH 8.0). The lipid-protein-cholate mixture was then frozen at -80°C for a minimum of 3 hours before being lyophilized. Following lyophilization, the particles were re-suspended in diethylpyrocarbonate (DEPC- RNAse inhibitor) treated water and dialyzed against PBS, for 2 days, with three buffer changes. The quantification of the siRNA incorporation into the rHDL particles was determined using RiboGreen assay (Quant-iT Ribogreen Kit, Cat no. R11490; Invitrogen,Carlsbad, CA).

rHDL Nanoparticle Characterization

Protein content of the rHDL nanoparticle was determined using a BCA Reagent Kit (Thermo Scientific). Phospholipid and cholesterol contents were determined using respective Phospholipid C and Cholesterol E kits respectively (Wako). Nanoparticle size determination was obtained via dynamic light scattering (performed on a MOBIUS dynamic light scattering (DLS) instrument by Dr. David Cistola's laboratory).

Stability Studies

A 5 mL sample of rHDL-siRNA nanoparticles was prepared, and characterized as the control sample. The stability of rHDL-siRNA nanoparticles was assessed by freezing and lyophilizing 1 mL aliquots of this preparation, and then storing them at either -20° or -80° for either two or four weeks. At the respective time points, the particles were re-suspended in 1 mL of DEPC treated water and the protein, phospholipid, cholesterol and siRNA contents as well as the particle diameter were determined.

Drug-rHDL Nanoparticle Preparation and Drug Incorporation

Imatinib Mesylate and Saquinavir (Sigma Aldrich, Saint Louis, MO) were dissolved in 1 mL of DMSO to produce stock solutions of 10 mg/mL. Next, a mixture of lipids (free cholesterol [FC]/cholesteryl oleate [CE]/egg yolk phosphatidylcholine [PC], in a molar ratio of 1:5:1.3:115) was dried under a stream of nitrogen. Following drying, either Imatinib Mesylate or Saquinavir (1 mg/mL) was added to the preparation along with Apo-A1 (2.5mg/mL). Sodium cholate, 140 μl (100 mg/ml stock in PBS was added to produce a final PC-to-cholate molar ratio of ~1:1.6, and the final volume was adjusted to 2 ml with buffer (10 mM Tris, 0.1 M KCl, 1 mM EDTA pH 8.0). The nanoparticles were incubated at 4°C for 12 hours, and then dialyzed against PBS for 2 days with three buffer changes. Imatinib Mesylate incorporation was determined using a free drug standard curve via absorption spectrophotometry at 260 nm, after subtraction of an empty nanoparticle control value to account for the absorption effect of the protein component. Saquinavir incorporation was determined using a free drug standard curve via fluoromery (Excitation: 250 nm, Emission: 400 nm). Dynamic Light Scattering for size distribution was performed using a Nanotrac system (Microtrac Inc., Montgomeryville, PA, USA) in Dr. Jamboor K. Vishwanatha's lab.

Cell Culture Conditions

SJ-N-KP and IMR-5 neuroblastoma cell lines were generous gifts from Dr. Fabio Timeus (Torino Children's Hospital/University of Turin, Turin Italy). SKOV-3 ovarian cancer cells were obtained from the ATCC. SKOV-3, SJ-N-KP and IMR-5 cells were all maintained in RPMI-1640 with 10% FBS and 1% penicillin-streptomycin (Gibco: Life Technologies).

Delivery of siRNA and Knockdown of the Target Gene

These proof of concept studies were performed to evaluate the ability of the rHDL nanoparticles to deliver siRNA to the cells. The knockdown of the expression of the target protein (SR-B1) was tested in the ovarian cancer cell line SKOV-3 based on previous studies showing high level of SR-B1 expression by these cells [15]. SKOV-3 cells were counted using a hemocytometer and 60,000 cells were plated in each well on a 12 well culture plate in RPMI-1640 medium + 10% FBS and incubated overnight at 37°C and 5% CO2. After incubation, either no siRNA (negative control) or one of two siRNA treatments of the cells was used. For the first treatment (positive control) 24 µL (2 µL per well) of Lipofectamine RNAimax reagent (Invitrogen) was diluted to 100 µL in Opti-MEM media (Invitrogen) and mixed with 144 pM (12 pM per well) SR-B1 targeting siRNA (also diluted to 100 µL in Opti-MEM media) and incubated for 15 minutes at room temperature before being added to the cells. For the second treatment, 10 ng rHDL-siRNA was added directly to the cells. The treated cells were incubated for either 24 or 48 hours. Following incubation, the knockdown of the rHDL-siRNA was compared to the knockdown efficiency of the Lipofectamine RNAiMAX transfection kit using Western blots. SDS-PAGE was run at 100 V for 45-60 minutes on 10% acrylamide, gradient gels (Bio-Rad Laboratories, Hercules, CA, USA). The protein was subsequently transferred to PVF membranes overnight at 40V and 4°C for western blot analysis). Membranes were probed for SR-B1 content using a primary rabbit monoclonal antibody for the SR-B1 receptor followed by a secondary rabbit polyclonal antibody (Ab-cam, Cambridge, MA).

Cytotoxicity Assays

The effects of Saquinavir and Imatinib as free drugs and encapsulated in rHDL nanoparticles were compared using the CCK-8 kit (Dojindo Molecular Technologies, Tabaru, Japan). Briefly, the neuroblastoma cell lines SJ-N-KP and IMR-5 were grown in RPMI-1640 with Glutamine and 10% FBS, and incubated at 37°C and 5% CO_2 (2). Cells were loosely attached to the flasks, so the cells were passaged in their own media. Cells were counted using a hemocytometer and 5000 cells were seeded per well into a 96-well micro-titer plate and then incubated at 37°C in 5% CO_2 for 24 hours. The free drug and the rHDL nanoparticles were diluted in PBS to yield stock solutions of equivalent molar concentrations. Subsequently, aliquots of the respective (saquinavir and imatinib-mesylate) stock solutions were added to the micro-titer plate wells to achieve the selected concentrations of 0.1, 0.5, 1, 2 and 5 µM of the drugs for the cell viability tests. Controls included cells with media (without rHDL/drug), and media without cells with the same rHDL/drug and free drug of each concentration used. Cells were incubated at 37°C in 5% CO_2 for 48 hours. After incubation,10 µL of the CCK-8 reagent (highly water-soluble tetrazolium salt, WST-8[2-(2-methoxy-4-nitrophenyl)-3-(4-nitrophenyl)-5-(2,4- disulfophenyl)-2H-tetrazolium,monosodiumsalt]stock solution) was added to each well. After 3 hours of incubation at 37°C, the absorbance at 450nm was measured using a Bio-Rad3550 microtiterplate reader (Bio-Tek Winooski, VT). Cytotoxicity at each concentration was determined using four replicates.

CHAPTER III

RESULTS

Optimization of rHDL-siRNA Nanoparticles

Based on, previous studies using rHDL-paclitaxel nanoparticles for enhanced treatment of breast, prostate and ovarian cancers [17]; we perceived a potential problem for clinically acceptable formulations regarding the heterogeneity of the main lipid component: egg-yolk phosphatidylcholine (EYPC). To overcome this problem, we tested seven different synthetic phospholipids to evaluate their respective impacts on the chemical composition and drug incorporation abilities of the resulting rHDL nanoparticles. These synthetic phosphatidylcholines were chosen, based on their fatty acid chain length and degree of unsaturation (Figure 4). The different preparations were then analyzed for their chemical composition, paclitaxel incorporation, size distribution and homogeneity. Compositional studies were performed using commercial kits for Phospholipid C, Cholesterol E, and BCA. Paclitaxel incorporation was determined using a scintillation counter via isotope dilution calculations. Particle size distribution was determined using dynamic light scattering. Table 1 shows the respective contributions of the protein, phospholipid, cholesterol and paclitaxel components of each formulation, while Figure 5 shows the composition ratios for each. The most important of these is the ratio between Apo-AI and the phospholipid component that was earlier suggested to influence the interaction of the nanoparticle with the targeted Sr-B1 receptor. Based on these earlier findings a Protein: Phospholipid ratio between 1-1.5 to 1-3 was considered optimal for the

targeting ability of Apo-AI. Accordingly, we eliminated the DSPC and DMPC preparations from consideration. However, regarding percent incorporation (Figure 6), the EYPC based nanoparticles showed almost double the incorporation of that of the best synthetic phospholipid: 1,2 dioleoylphosphatidylcholine. Due to the large drop in paclitaxel incorporation efficiency with the use of synthetic phospholipids, we decided to maintain use of EYPC as our main lipid component for the rHDL-nanoparticles.

Subsequently, we changed our focus to concentrate on the rHDL-siRNA nanoparticles. First, formulations using the best synthetic phospholipid found from figures 5 and 6 (DOPC), a different naturally based phospholipid, soybean phosphatidylcholine (SBPC) and the control EYPC (Table 2) were investigated. These data show only minor differences in physiochemical properties, composition and siRNA incorporation among the respective formulations tested (Figure 7 and 8). On the other hand, variations in the levels of Apolipoprotein A-I or Apo-AI (Figure 9) show a negative correlation between the loading efficiency of siRNA and the initial concentration of Apo A-I.

Once the best formulation of physiochemical properties for rHDL-siRNA was determined, different formulation processes were investigated. No major changes were found regarding siRNA incorporation and nanoparticle composition when low and high salt dialysis buffers were compared (Figure 10). Inclusion of a lyophilization step before the dialysis in the preparative process yielded no major changes in particle composition (Figure 11), however it yielded a more homogeneous nanoparticle preparation compared to the one without lyophilization (Figure 12).

Stability Studies with Optimized rHDL-siRNA Nanoparticles

Nanoparticles made with the best formulation were subsequently lyophilized and stored at either -20°C or -80°C for two and four weeks to determine their stability. These stability studies for rHDL-siRNA preparations (Figure 13 and 15) showed no change in the composition or in the siRNA levels of the nanoparticles. Dynamic light scattering studies (Figure 14), however, revealed the appearance of larger diameter particles, resulting in a more heterogeneous preparation.

Cellular uptake via rHDL-siRNA compared to a Lipofectamine Transfection kit

The Uptake of rHDL-siRNA by target cells by SKOV-3 ovarian cancer cells was compared to that of a standard Lipofectamine RNAiMAX Transfection kit. A concentration of 10 ng of SR-B1 siRNA directed against the SR-B1 receptor protein was delivered either via rHDL or Lipofectamine complex for time periods of 24 hours and 48 hours. Western Blot analysis for both time points (Figures 16-17) show higher knockdown via delivery with rHDL-siRNA compared to the findings obtained via the use of the Lipofectamine complex. These results show that the rHDL-siRNA nanoparticles are highly efficient in delivering siRNA to target cells resulting in the knock down of the protein of interest.

1,2 dimyristoyl-*sn*-glycero-3-phosphocholine:

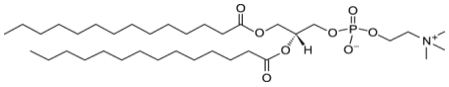

1,2 dipalmitoyl- *sn*-glycero-3-phosphocholine:

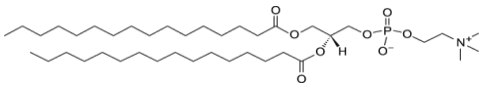

1,2 distearoyl- *sn*-glycero-3-phosphocholine:

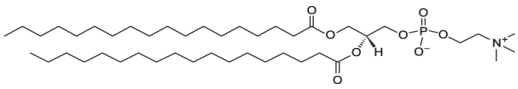

1,2 dioleoyl- *sn*-glycero-3-phosphocholine:

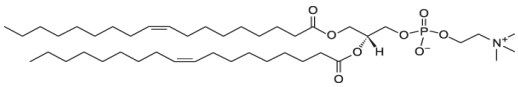

1-palmitoyl, 2-oleoyl- *sn*-glycero-3-phosphocholine:

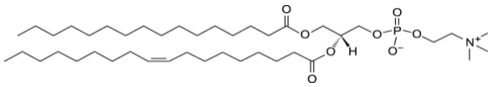

1,2-dilinoleoyl-*sn*-glycero-3-phosphocholine:

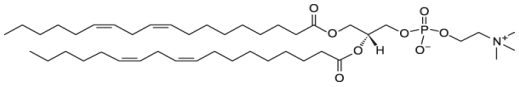

1,2-diarachidonyl-*sn*-glycero-3-phosphocholine

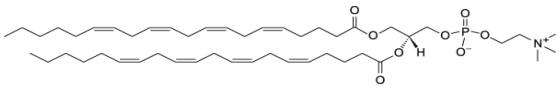

Figure 4. Structures of phospholipids used to prepare rHDL-paclitaxel preparations.

	Protein	**Phospholipid**	**Cholesterol**	**Drug**	**Total (mg/ml)**
EYPC-empty	0.36	2.14	0.07	0	2.57
EYPC-ptx	0.64	3.19	0.12	0.41	4.36
DOPC-ptx	0.4	1.29	0.15	0.19	2.03
POPC-ptx	0.47	1.85	0.21	0.13	2.66
DPPC-ptx	0.33	0.7	0.11	0.04	1.18
DMPC-ptx	0.4	3.14	0.11	0.12	3.77
DAPC-ptx	0.43	1.4	0.17	0.07	2.07
DLPC-ptx	0.75	1.17	0.11	0.07	2.1

Table 1: Chemical compositions (mg/mL) of the rHDL-paclitaxel particles made with one of the seven synthetic phospholipids and with EYPC (control).

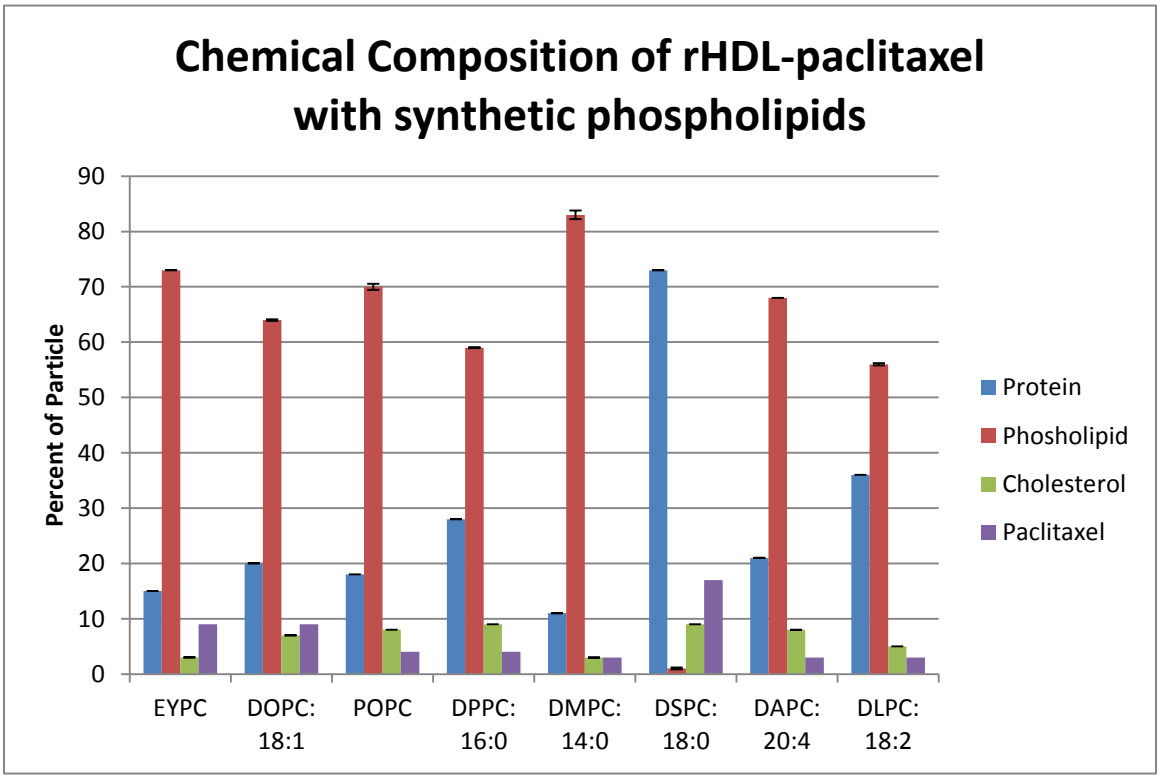

Figure 5. Composition of rHDL-paclitaxel nanoparticles made with the different synthetic phospholipids and EYPC. Error bars represent SD. n=2.

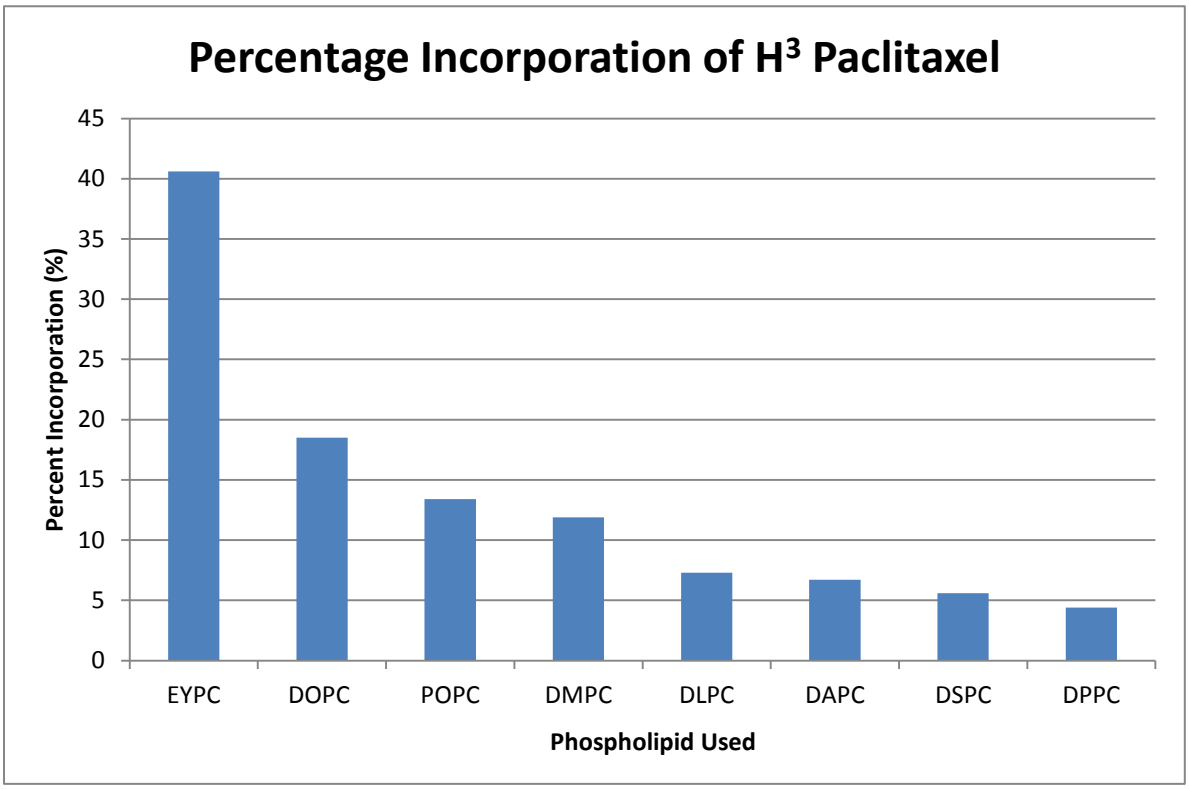

Figure 6. Incorporation of Paclitaxel into rHDL-paclitaxel nanoparticles prepared with different synthetic phospholipids and EYPC. Numbers are based on a comparison of the final scintillation counts for the compared to the initial paclitaxel readings.

	Protein	Phospholipid	Cholesterol	siRNA	Total
EYPC	0.88	1.505	0.0695	0.0095	2.459
DOPC	1.47	2.15	0.07	0.011	3.701
SBPC	1.64	1.9	0.107	0.01	3.657

Table 2. Chemical Composition (mg/mL) of the rHDL-siRNA nanoparticles made with the DOPC, SBPC or and EYPC. Numbers represent an average of 3 different samples.

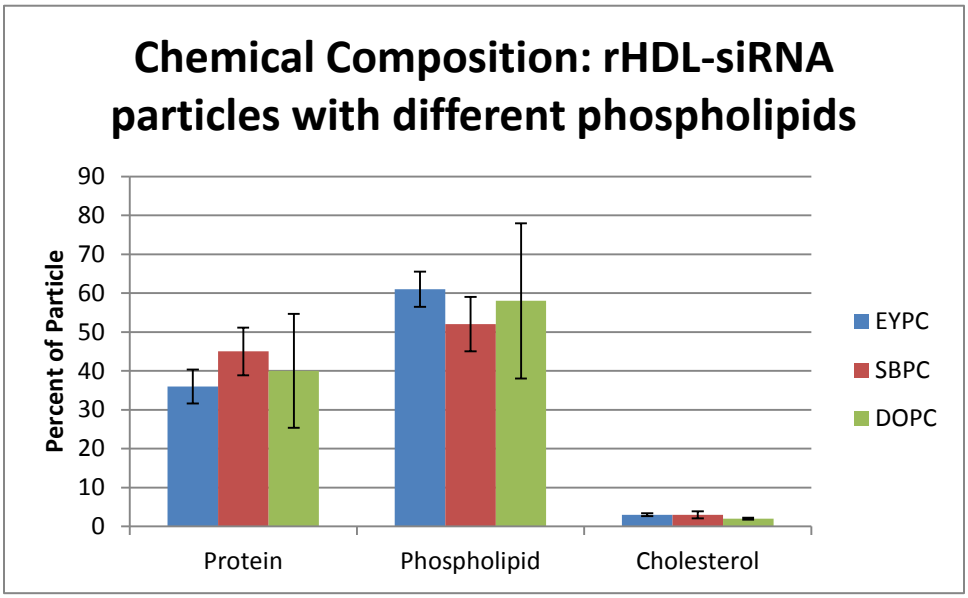

Figure 7. Composition of rHDL-siRNA nanoparticles made with DOPC, SBPC and EYPC. Numbers represent findings for an average of 3 different preparations. Error bars represent SEM. n=2.

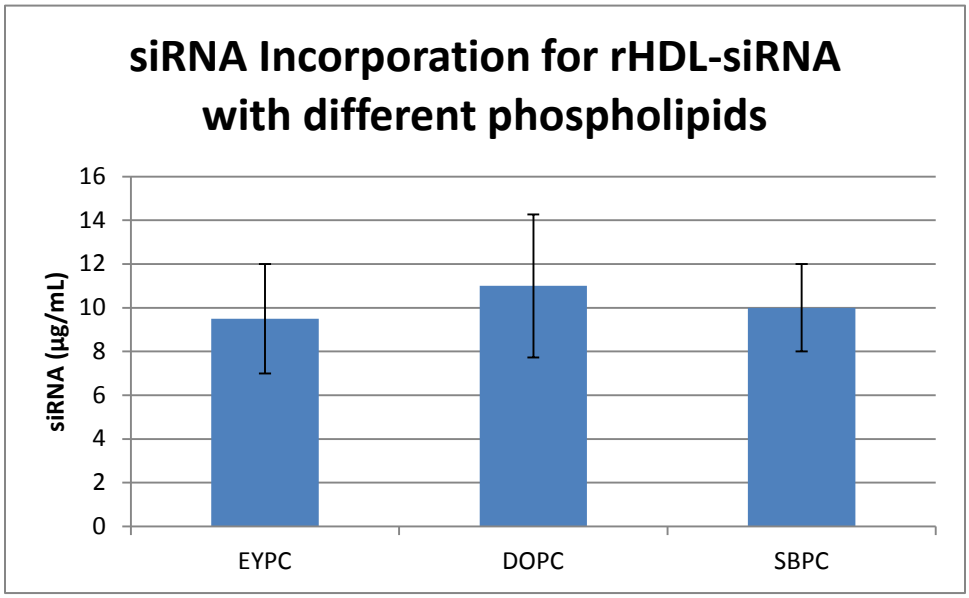

Figure 8. siRNA incorporation into rHDL-siRNA nanoparticles prepared with DOPC, SBPC and EYPC. The data represent an average of 3 different determinations. Bars represent SEM; n=2.

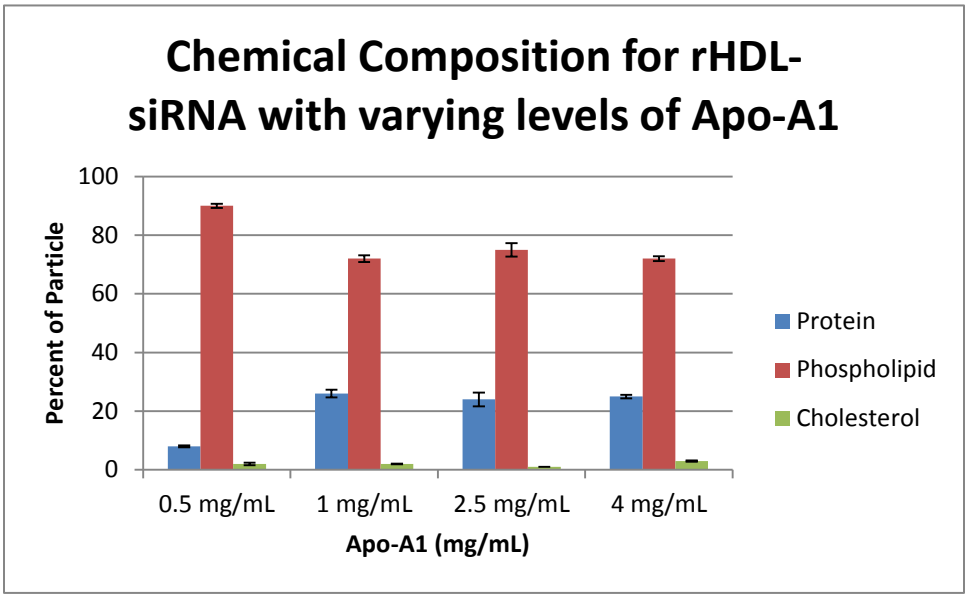

Figure 9. Composition of rHDL-siRNA nanoparticlesprepared with increasing initial amounts of Apo-AI. Error bars represent SD. n=2.

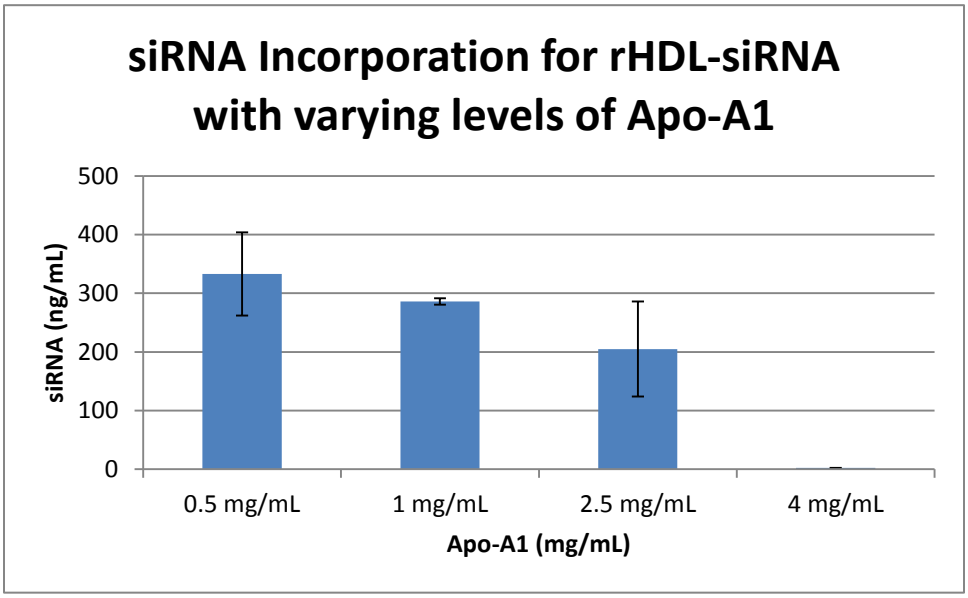

Figure 10. siRNA into rHDL-siRNA nanoparticles prepared with increasing initial amounts of Apo-AI. Error bars represent SD; n=2.

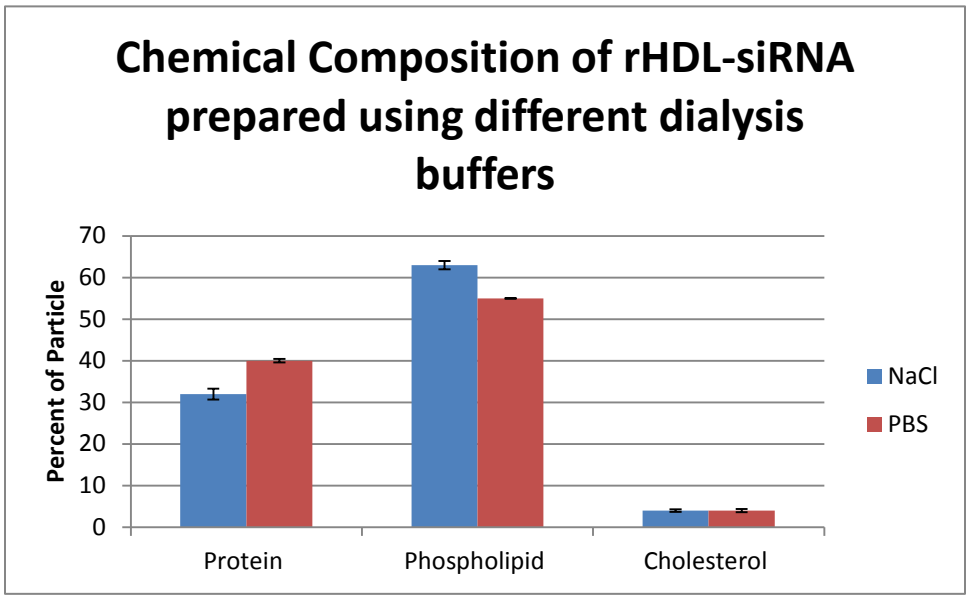

Figure 11. Composition of rHDL-siRNA nanoparticles prepared using different dialysis buffers. The NaCl sample was prepared using a high salt (NaCl) buffer for the first 2 hours of cholate dialysis, before changing back to the control buffer (PBS) for the remainder of dialysis. Error bars represent SD. n=2.

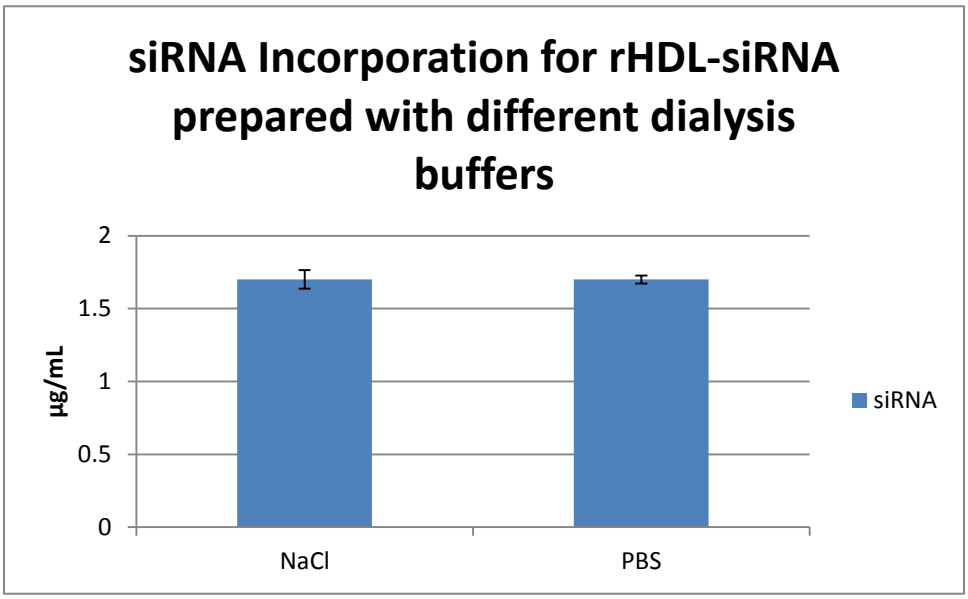

Figure 12. siRNA incorporation into rHDL-siRNA nanoparticles prepared using different dialysis buffers. The NaCl sample was prepared using a high salt (NaCl) buffer for the first 2 hours of cholate dialysis, before changing back to the to the control buffer (PBS) for the remainder of dialysis. Error bars represent SD; n=2.

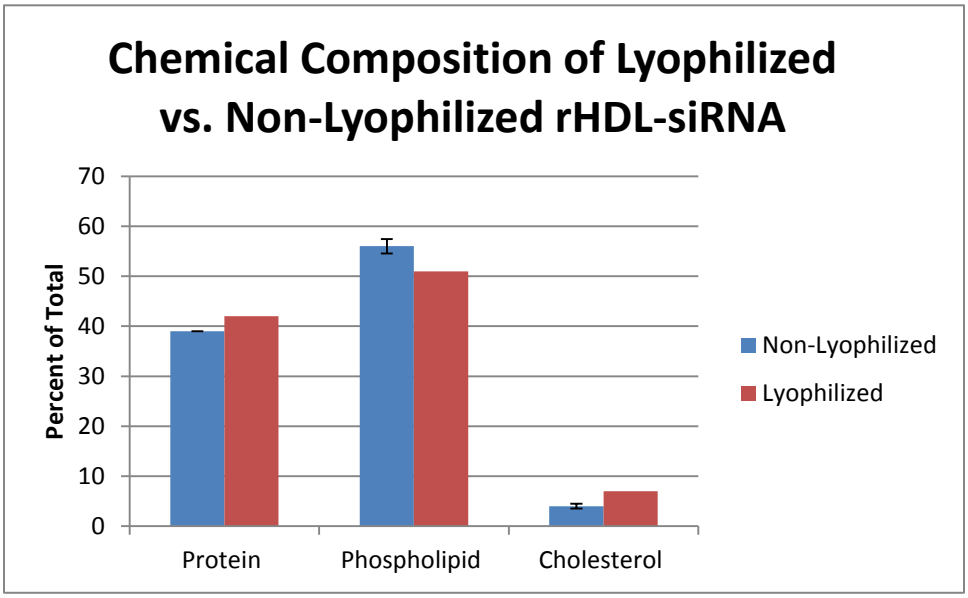

Figure 13. Composition of rHDL-siRNA nanoparticles prepared with or without the additional lyophilization step before cholate dialysis. Error bars represent SD. n=2.

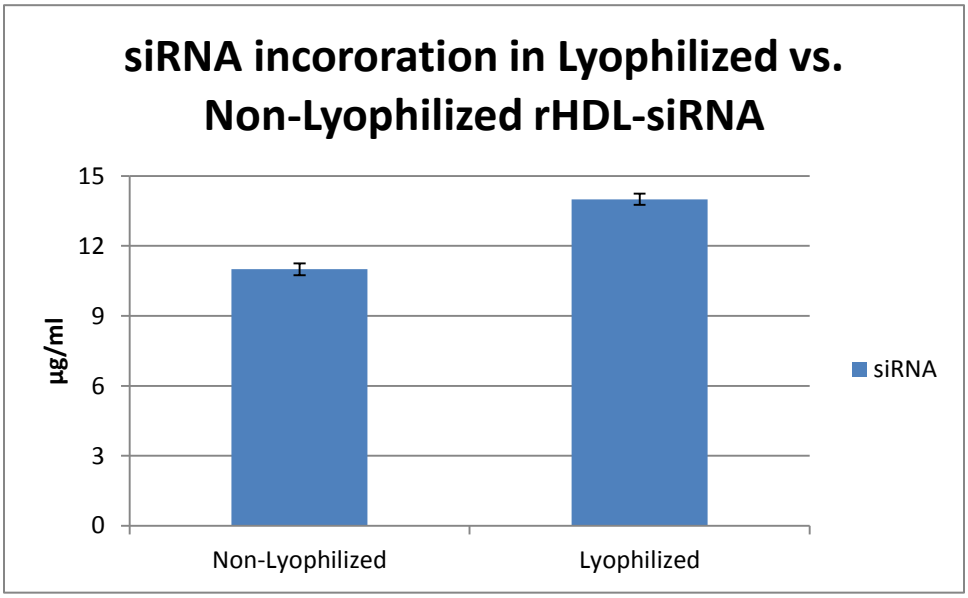

Figure 14. siRNA incorporation into rHDL-siRNA nanoparticles prepared with or without the additional lyophilzation step before cholate dialysis. Error bars represent SD; n=2.

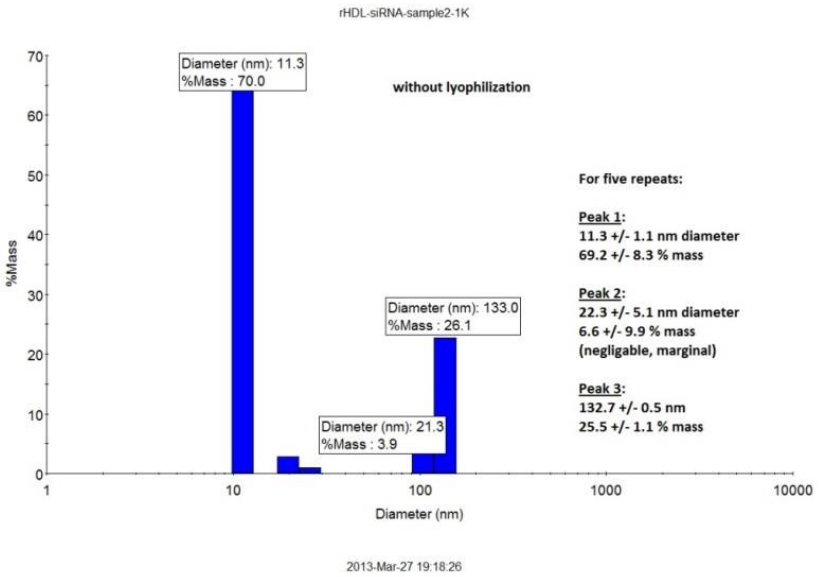

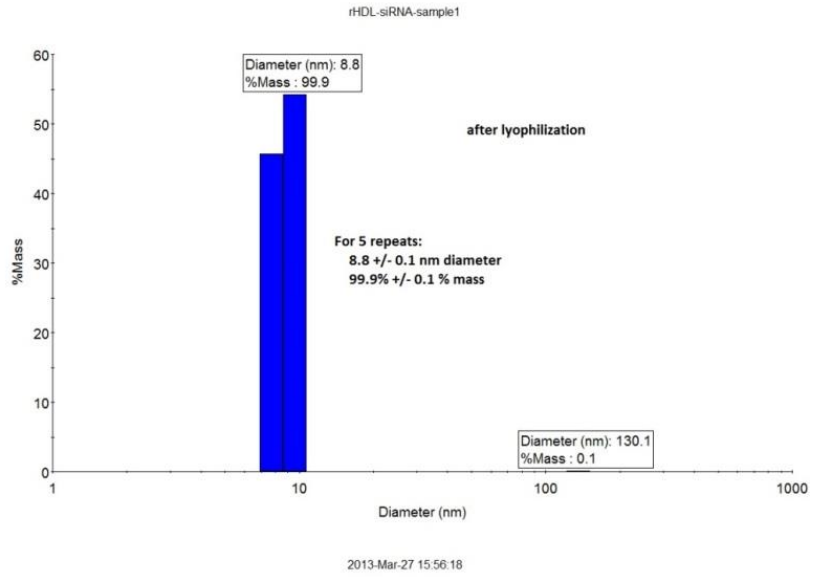

Figure 15 (a &b). Dynamic light scattering analysis of particle size distributions for rHDL-siRNA nanoparticles prepared with (a) or without (b) the additional lyophilization step before cholate dialysis. Analysis was performed on a MOBIUS dynamic light scattering instrument by Dr. David Cistola.

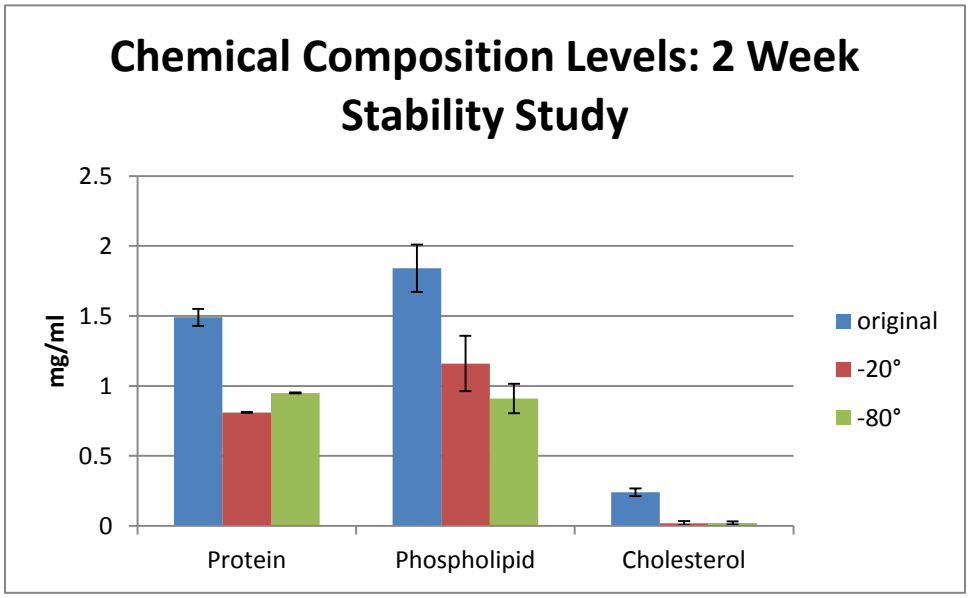

Figure 16. Composition of rHDL-siRNA nanoparticles stored for 2 week stability studies. These nanoparticles were frozen and re-lyophilized in 1 mL aliquots, and then stored at either -20°C or -80°C for 2 weeks. After 2 weeks, the aliquots were re-suspended in 1 mL of DEPC treated water and analyzed for composition again. Error bars represent SD; n=2.

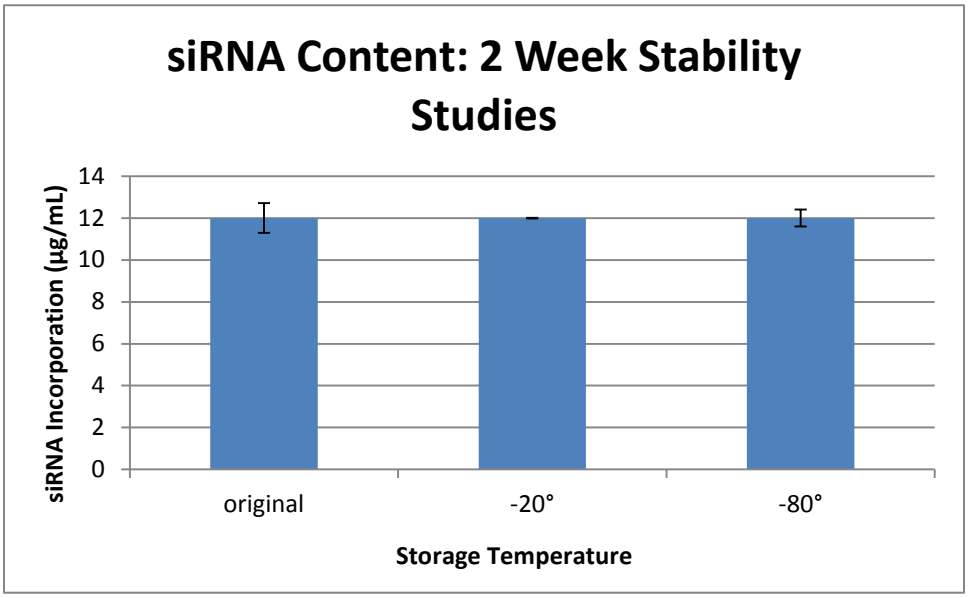

Figure 17. siRNA incorporation into rHDL-siRNA nanoparticles stored for 2 week stability studies. These nanoparticles were frozen and re-lyophilized in 1 mL aliquots and then stored at either -20°C or -80°C for 2 weeks. After 2 weeks, the aliquots were re-suspended in 1 mL of DEPC treated water and analyzed for their siRNA levels. Error bars represent SD; n=2.

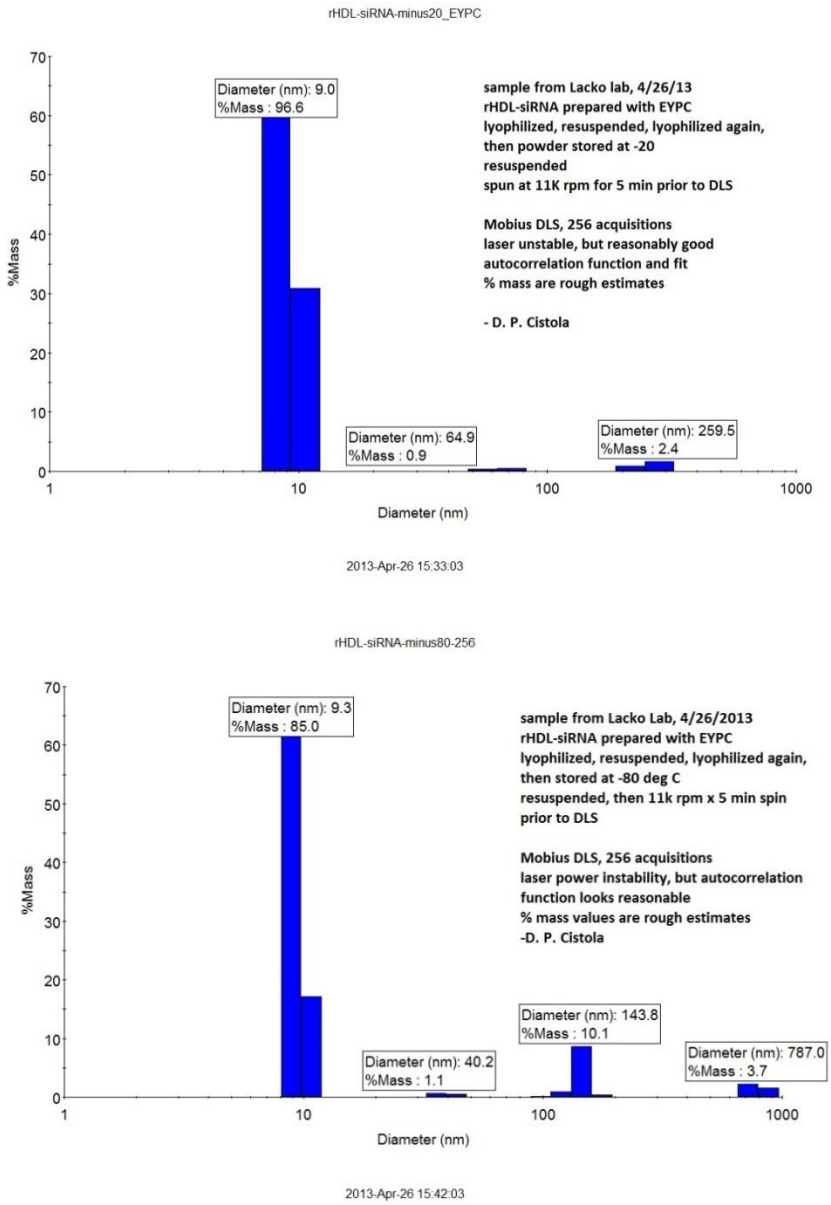

Figure 18 (a &b). Dynamic light scattering analysis of particle size distributions for rHDL-siRNA nanoparticles. The siRNA containing nanoparticles were prepared, frozen and re-lyophilized in 1 mL aliquots. These aliquots were stored at either a) -20°C or b) -80°C for 2 weeks. After 2 weeks, the aliquots were re-suspended in 1 mL of DEPC treated water and analyzed again. DLS analysis was performed on a MOBIUS dynamic light scattering instrument by Dr. David Cistola.

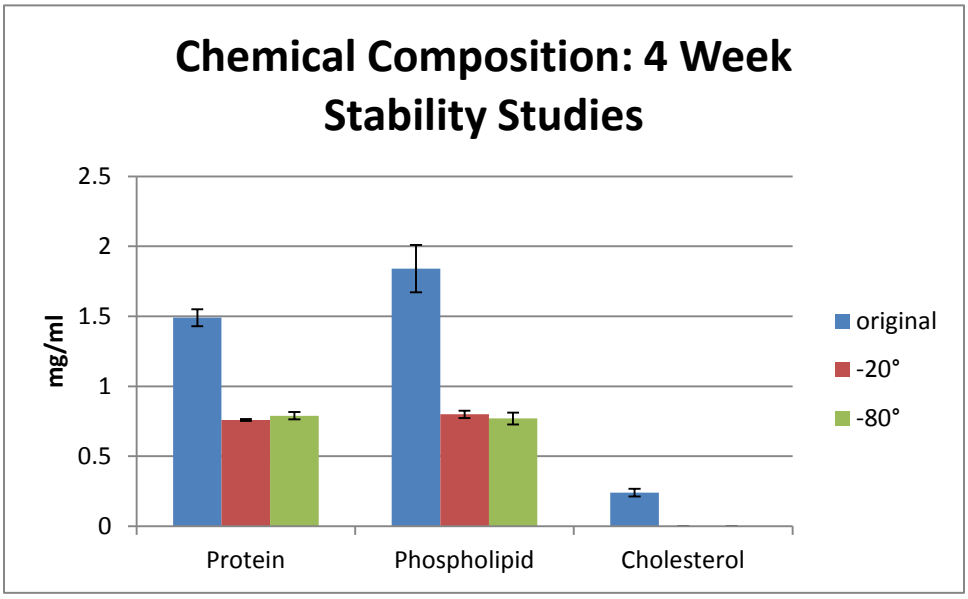

Figure 19. Composition of rHDL-siRNA nanoparticles prepared, and stored for 4 week stability studies. The samples were frozen and re-lyophilized in 1 mL aliquots. These aliquots were stored at either -20°C or -80°C for 4 weeks. After 4 weeks, the aliquots were re-suspended in 1 mL of DEPC treated water and analyzed for composition levels again. Error bars represent SD. n=2.

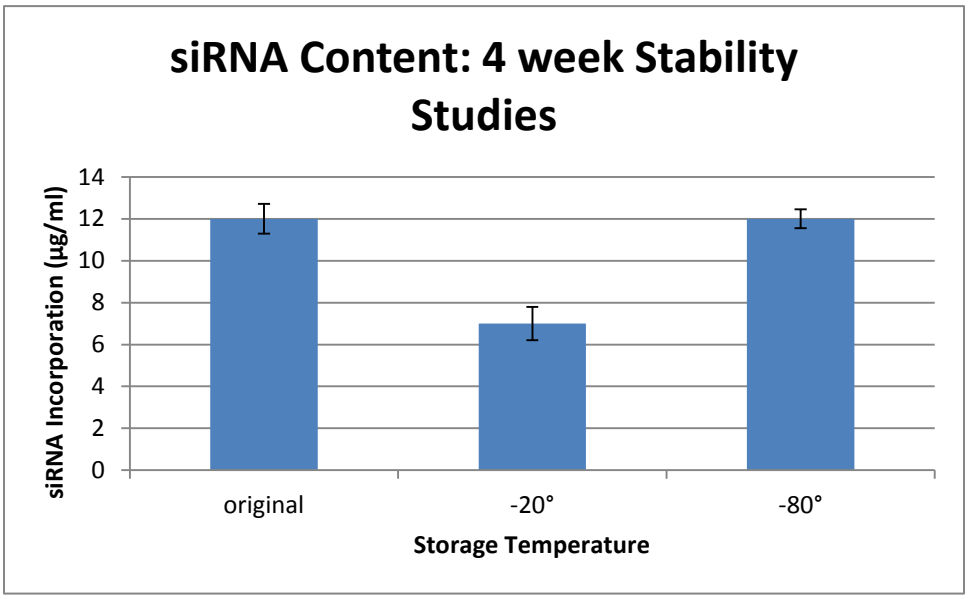

Figure 20. siRNA incorporation into rHDL-siRNA particles prepared, frozen and re-lyophilized in 1 mL aliquots. These aliquots were stored at either -20°C or -80°C for 4 weeks. After 4 weeks, the aliquots were re-suspended in 1 mL of DEPC treated water and analyzed for their siRNA levels. Error bars represent SD; n=2.

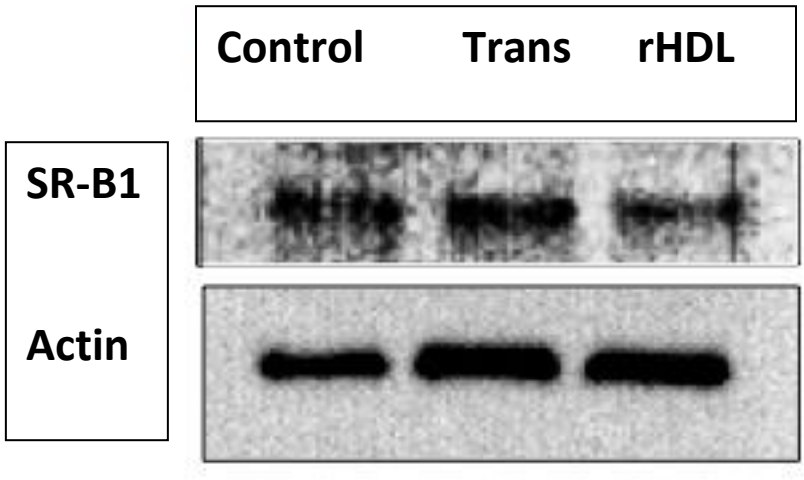

Figure 21. Western Blot Analysis of rHDL-siRNA vs. Lipofectamine 24 hours after transfection. SKOV-3 cells were plated and incubated overnight at 37°C and 5% CO_2. After incubation, one of 3 treatments was applied: no treatment (negative control), the addition of siRNA-Lipofectamine complexes via Lipofectamine RNAiMAX transfection kit (positive control) and the addition of rHDL-siRNA. Upon treatment, cells were incubated for 24 hours. Following incubation cells were lysed and SDS-PAGE and Western Blot analysis were performed.

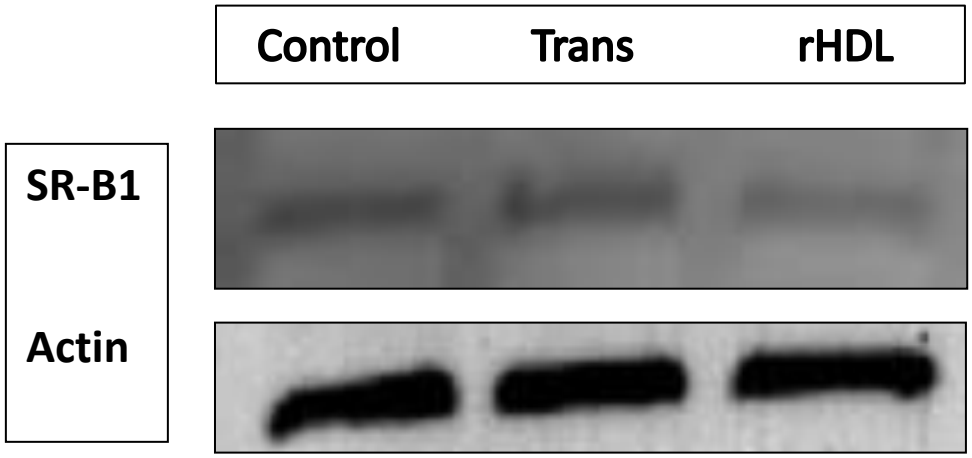

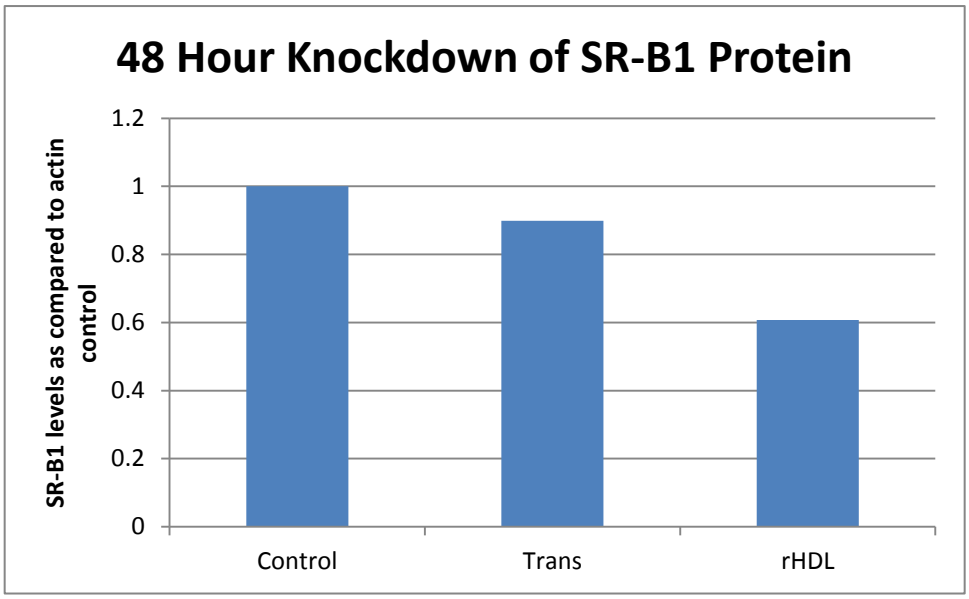

Figure 22 a & b. a) Western Blot Analysis of rHDL-siRNA vs. Lipofectamine 48 hours after transfection. SKOV-3 cells were plated and incubated overnight at 37°C and 5% CO_2. After incubation, one of 3 treatments was applied: no treatment (negative control), the addition of siRNA-Lipofectamine complexes via Lipofectamine RNAiMAX transfection kit (positive control) and the addition of rHDL-siRNA. Upon treatment, the cells were incubated for 48 hours. Following incubation cells were lysed and SDS-PAGE and Western Blot analysis were performed. b) Quantification of western blot analysis using densitometry, and normalized to the Actin control. (n=1)

CHAPTER IV

Characterization of rHDL-Imatinib and rHDL-Saquinavir nanoparticles

rHDL-Imatinib and rHDL-Saquinavir nanoparticles were prepared by the standard cholate dialysis method [15], and subsequently characterized for chemical composition (Figure 23 and 25). Dynamic Light Scattering analysis was performed to determine the size distributions of the respective nanoparticles (Figure 24 and 26). rHDL-Saquinavir showed much more efficient drug incorporation and overall particle formation than rHDL-Imatinib (Figure 27). Both drugs allowed the preparation of drug containing nanoparticles for cytotoxicity analysis against NB cells.

Cytotoxicity Studies using rHDL-Imatinib and rHDL-Saquinavir against NB Cells

Cytotoxicity studies were performed using the CCK8 (Cell Counting Kit-8) Assay following 48 hour exposure of either free Imatinib, rHDL-Imatinib, free Saquinavir, or rHDL-Saquinavir against the IMR-5 and SJ-N-KP Neuroblastoma cell lines. rHDL-Saquinavir showed up to a 10 fold increase in cytotoxicity over free Saquinavir on SJ-N-KP cells (Figure 28), as determined by their IC-50 values. SJ-N-KP cells showed increased sensitivity to rHDL-Imatinib than did the IMR-5 cells (Figure 29), and both showed increased efficacy when compared to IC-50 values found by Dr. Timeus of: 2.79 µM for SJ-N-KP and 2.14 µM for IMR-5 cells [2].

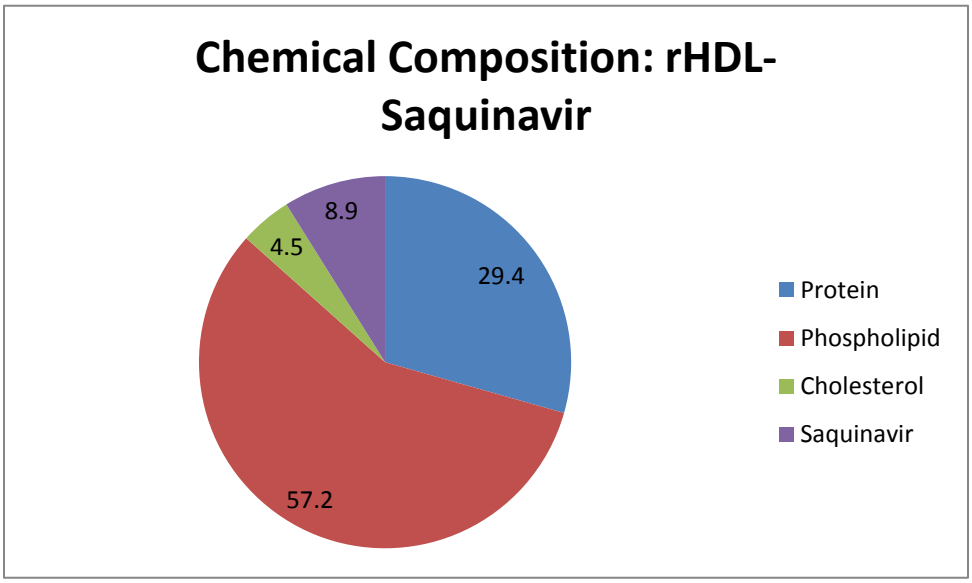

Figure 23. Chemical composition of rHDL-Saquinavir nanoparticles. The data represent average values for 6 different determinations.

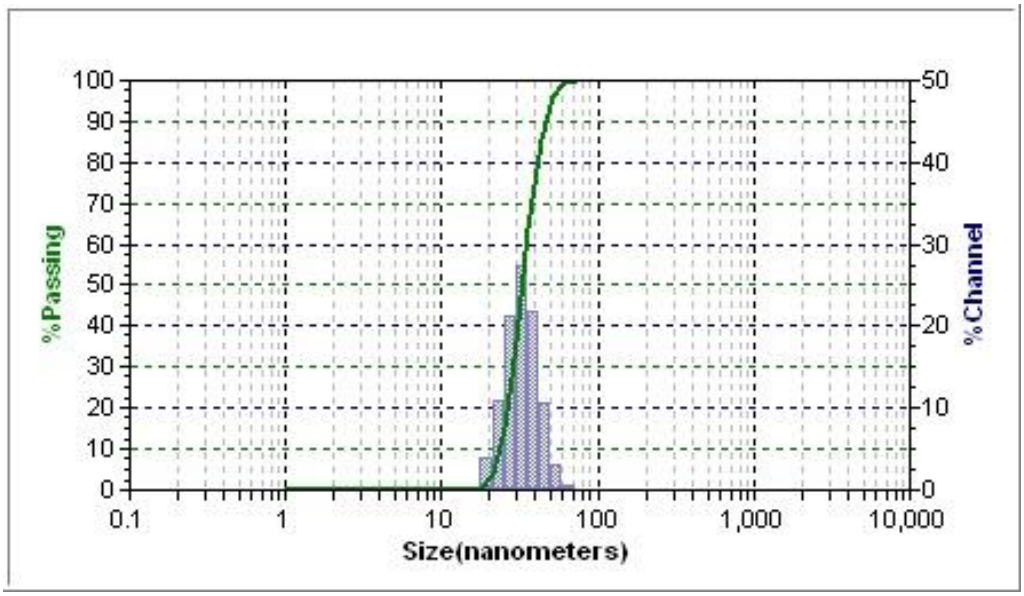

Figure 24. Dynamic light scattering analysis of particle size distribution rHDL-Saquinavir nanoparticles. Average diameter (33.1 nm). This analysis was performed using a Nanotrac system (Microtrac Inc., Montgomeryville, PA, USA) in Dr. Jamboor K. Vishwanatha's lab..

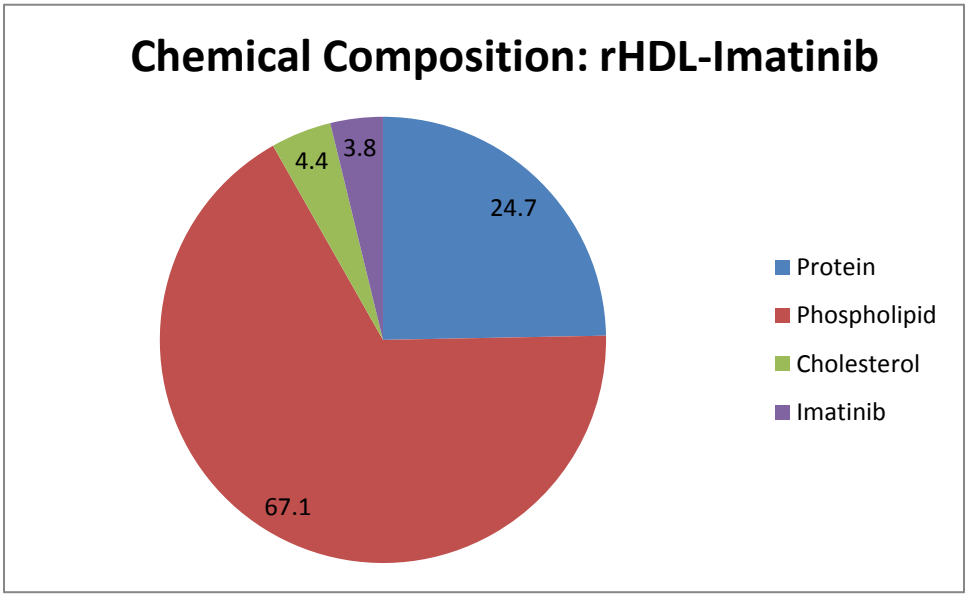

Figure 25. Chemical composition of rHDL-Imatinib nanoparticles. The data shown represent average values for 6 separate determinations.

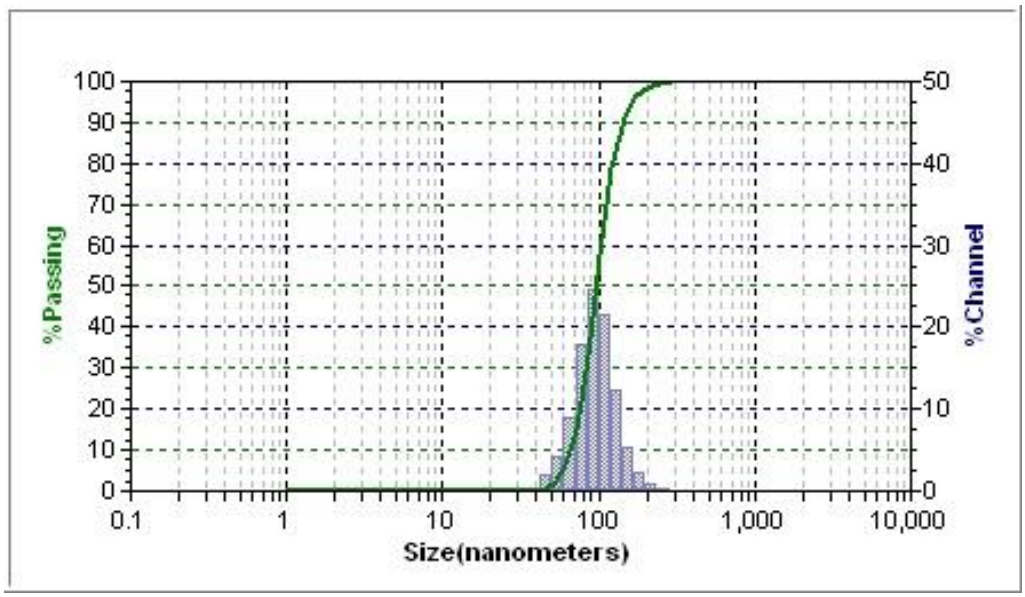

Figure 26. Dynamic light scattering analysis of particle size distribution of rHDL-Imatinib nanoparticles. Average diameter (97.1 nm). This analysis was performed using a Nanotrac system (Microtrac Inc., Montgomeryville, PA, USA) in Dr. Jamboor K. Vishwanatha's lab.

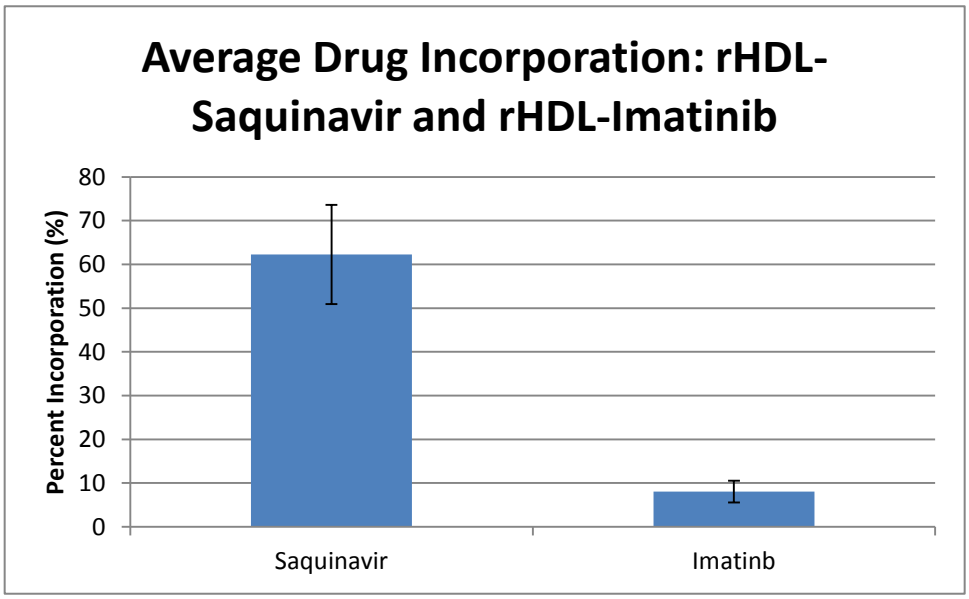

Figure 27. Drug incorporation efficiency for rHDL-Saquinavir and rHDL-Imatinib nanoparticles. Saquinavir concentration was assessed by was fluorometry. (Exc: 250 and Em: 400). Data for rHDL-Imatinib concentrations were estimated by spectrophotometry. Absorbance = 260nm. rHDL-Imatinib content was assessed by subtracting the empty nanoparticle absorbance from the total reading. Averages values shown are based on 6 different determinations. Error bars represent SEM; n=2.

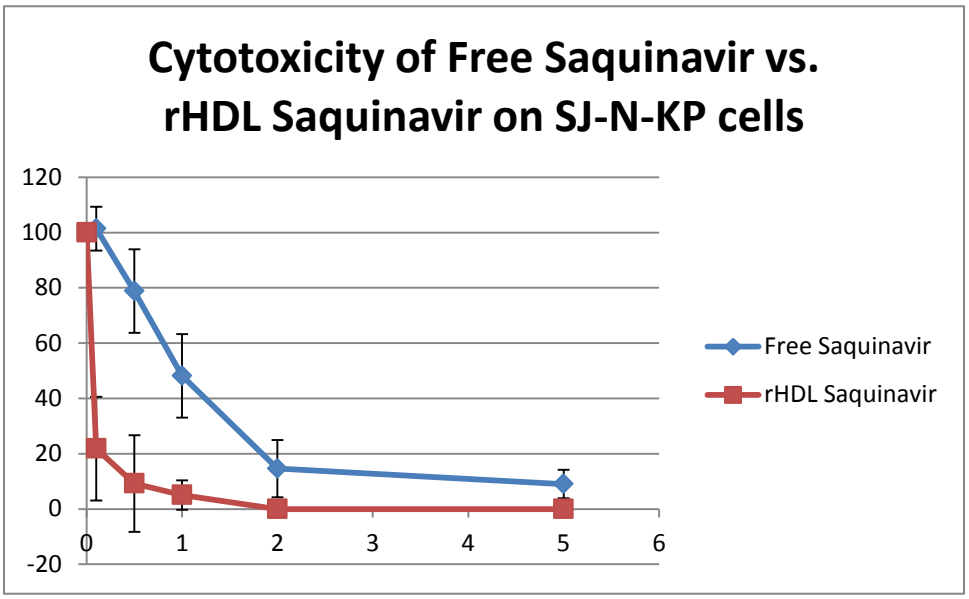

Figure 28. SJ-N-KP (NB) cell viability after 48 hour incubation with increasing concentrations of either free Saquinavir or rHDL-Saquinavir. Error bars represent SD; n=4.

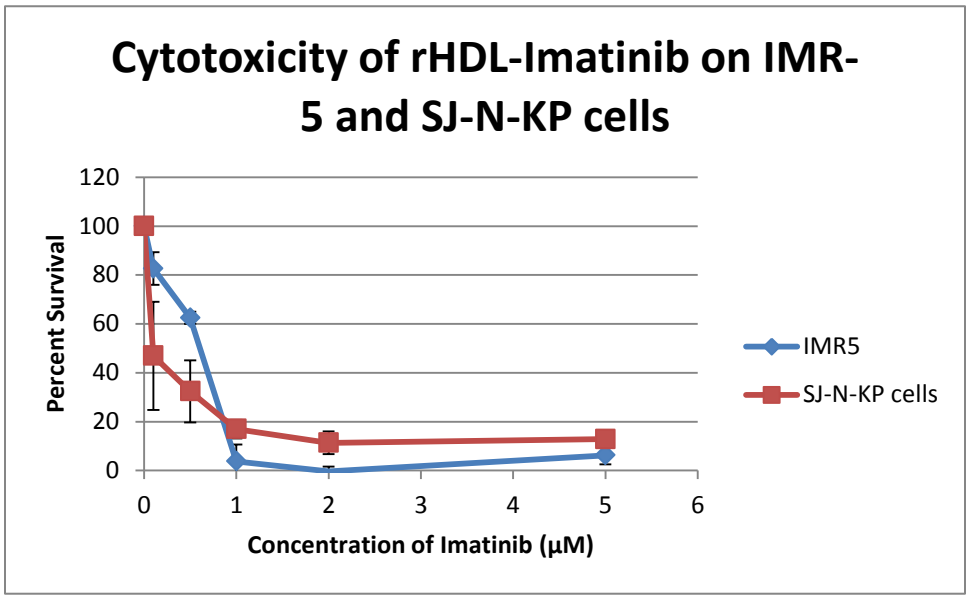

Figure 29. SJ-N-KP and IMR-5(NB) cell viability after 48 hour incubation with increasing concentrations of rHDL-Imatinib. Error bars represent SD; n=4.

CHAPTER V

DISCUSSION

Nanoparticles have been employed for the delivery of anti-cancer agents for the last two decades to overcome the poor pharmacokinetics that limits the efficacy of numerous chemotherapeutic agents. Reconstituted HDL (rHDL) is a nanoparticle with particularly favorable characteristics for therapeutic delivery of drugs because it can overcome not only poor solubility and bioavailability, but it also has the potential to overcome toxic side effects, and drug resistance. The key to overcoming these obstacles via rHDL nanoparticles is the apolipoprotein A-I (Apo A-I) content of the drug/lipoprotein complex that facilitates the receptor (SR-B1) mediated uptake and thus the tumor selective delivery of drugs. The amphipathic nature of Apo A-I also facilitates its combination with phosphatidylcholine (PC) and thus allows for the formation of a hydrophobic inner core to encapsulate lipophilic drugs. Simultaneously, the hydrophilic outer shell renders the rHDL nanoparticles water soluble for effective systemic administration and transport capacity. Through this selective tumor targeting mechanism, the peripheral toxicities of the anti-cancer agents are anticipated to be dramatically decreased, leading to an improved quality of life for patients undergoing cancer chemotherapy. The optimization of these particles for improved drug encapsulation, and delivery to the cancer cells is an essential step for advancing the rHDL nanoparticle formulation toward clinical applications.

The first goal of this project was to determine the effects of individual synthetic phospholipids, on the chemical composition and drug incorporating capacity of the rHDL nanoparticles, as compared to the control: naturally derived phospholipid mix, EYPC. First we examined rHDL-paclitaxel nanoparticles based on previous findings in our lab [17]) ,prepared with seven synthetic phospholipids (Figure 4) as compared to \ a natural mix of (egg-yolk) phosphatidylcholine. The particles made with the synthetic phospholipids showed significantly lower drug incorporation efficiency, the highest being only about half of that of the EYPC control (Figure 6). It is likely that some of the relative inefficiency of drug incorporation by the synthetic PC species based nanoparticles was due to the differing transition temperatures for each PC. Interestingly the arachidonyl PC species ahowed one of the lowest efficiencies despite its lower transition temperature. Nevertheless, the transition temperatures could be important for some of the PC species during cholate dialysis which drives the assembly of the nanoparticles. Cholate dialysis is performed at 4°C, therefore when comparing paclitaxel incorporation to transition temperatures we found that DOPC, POPC and DMPC with transition temperatures of -20°C, -20°C, and 23°C respectfully, exhibited the highest paclitaxel incorporation.

Subsequently, the focus of the project transferred to the characterization of the rHDL-siRNA particles. First we examined a synthetic phospholipid (DOPC) and another naturally derived phospholipid: soy-bean phosphatidylcholine (SBPC), and found no substantial differences in the siRNA incorporation (Figure 8). rHDL-siRNA nanoparticles made with SBPC displayed no differences in chemical composition either. However, while the average chemical compositions for the respective particles (prepared with DOPC) were similar to those of the control (EYPC) particles (Figure 7), substantial heterogeneity was found among the composition of the different preparations of DOPC rHDL-siRNA. DOPC phospholipid content ranged from

a low of 27% in one preparation to a high of 82% in another preparation. Neither of these indicates indicates a desired Apo-A1: PC ratio for rHDL nanoparticles which is preferred to be between 60 and 75% phospholipid. The 82% phospholipid particle has a low protein content level that lower the targeting via targeting of Apo-AI to the SR-B1 receptor.

Due to the lack of differences in the SBPC rHDL-siRNA nanoparticles and the composition heterogeneity with DOPC rHDL-siRNA nanoparticles, we decided to focus on enhancing the current EYPC formulations by examining the impact of the Apolipoprotein A-1 (Apo-A1) component. Variation of the Apo-A-1 content showed a negative correlation between Apo-A1 concentration and siRNA incorporation (Figures 9 a & b). Based on these data and the chemical composition data for the same particles, it was determined that the initial Apo-A1 concentration should be limited to 1 mg/mL for the nanoparticle assembly process.

Next we focused on the enhancement of siRNA incorporation through alternative preparation techniques. First, we employed a high salt (NaCl) concentrated dialysis buffer in an attempt to suppress the impact of the negative charges present in the siRNA, and therefore enhance the hydrophobic interactions to localize the siRNA in the core region of the rHDL nanoparticle and thus achieve better encapsulation. However, when compared to the normal cholate dialysis buffer (1x PBS), there was no difference in siRNA incorporation (Figure 12). Next we examined the effect of lyophilization of the particles before the cholate dialysis step. Here we found no differences in the chemical composition of the rHDL-siRNA nanoparticles (Figure 13). However the extra lyophilization step did substantially increase the efficiency of siRNA incorporation (Figure 14), and also facilitated the assembly of a much more homogeneous population of particles, where 99.9% of the particles in the preparation were

represented by HDL type, diameter of 8.8 nm particles) as compared to only 70% of 11.3 nm particles in the non-lyophilized preparation (Figure 15).

Once the optimal formulation process for the rHDL-siRNA nanoparticles was established, the nanoparticles were re-lyophilized and stored as a powder at either -20° C or -80° C for time periods of two and four weeks to test their stability. Subsequent to the storage periods, the particles were re-suspended in DEPC treated water and their properties determined. The particles showed relatively stable chemical compositions with only minor losses in phospholipid and protein (Figures 16), while siRNA levels were maintained after two weeks of storage (Figure 17). However after four weeks of storage, the aliquot stored at -20°C showed loss of about half its siRNA content lost (Figure 19). Also, at two weeks, the nanoparticle preparation showed increased heterogeneity and now contained a larger diameter species at both the -20° and -80° storage temperatures (Figure 18). We believe the appearance of the larger diameter species is due to the second lyophilization step subsequent to the assembly of the nanoparticles, indicating that further stability studies with and without this second lyophilization step are required to produce more homogeneous preparations.

In order to test the efficacy of the improved formulation of the rHDL-siRNA particles, they were administered to SKOV-3 ovarian cancer cells to test their ability to knock down the SR-B1 receptor protein. The knockdown efficiency obtained via the rHDL transfection was compared to that of a commercial transfection kit (Lipofectamine RNAiMAX). After a 24 hour exposure to either the rHDL-siRNA particles or the Lipofectamine-siRNA complexes, the western blot (Figure 21) shows that the rHDL-siRNA knockdown of the SR-B1 expression in the SKOV-3 cells was markedly lower than the control transfection kit. Similar results were observed at the 48 hour time point (Figure 22a and b). Further *in vitro* time points of 72 hours

and longer, as well as further animal studies are needed to confirm and expand this finding. However, these data show that the rHDL-siRNA particles could be of potential clinical use for targeted gene therapy in cancer patients. Use of these particles, would allow for a more personalized approach to cancer therapy, by targeting key genes that are up-regulated during carcinogenesis or metastasis. This personal approach to cancer therapy should greatly enhance the efficacy of the treatment, and allow for improved prognosis for survival and better quality of life for cancer patients in general and HRNB patients in particular.

Another phase of these studies involved the evaluation of the effect of two experimental drugs: Imatinib and Saquinavir as new therapeutic agents for Neuroblastoma. The average chemical compositions of the respective nanoparticles containing Imatinib and Saquinavir show proper Apo-A1: Phospholipid ratios (Figure 23 and 25). However, while Saquinavir is encapsulated at a high efficiency into the rHDL particles, (63%), Imatinib showed a much poorer encapsulation efficiency of (8%) (Figure 27). However, even with this low encapsulation efficiency, both rHDL-drug particles were found to be effective in suppressing the proliferative capacity of NB cells.

First we tested the drugs separately, both the encapsulated rHDL form and the free drug, on two different NB cell lines, IMR-5 and SJ-N-KP. Saquinavir was found to be highly effective both as the encapsulated drug and as the free forms against SJ-N-KP cells (Figure 28). The rHDL-Saquinavir proved to be over 10x more effective than free Saquinavir, with an IC_{50} less than 0.1 µM compared to the free drug IC_{50} around 1 µM. More detailed analyses may be needed below 0.1 µM in order to precisely assess the IC_{50} of the encapsulated drug preparation. Imatinib also proved to be highly effective against both SJ-N-KP cells and IMR-5 cells (Figure 29) with IC_{50} values around 0.1 and 0.75 respectively, however due to interference with the

absorption measurements involving the CCK-8 and MTT reagents, the effects of free Imatinib could not be accurately measured. While we could not determine directly the free Imatinib IC_{50}values, we were able to compare them to values published by Dr. Timeus' original study of 2.79 (SJ-N-KP) and 2.14 (IMR-5) [2]. Therefore the rHDL-Imatinib preparation did prove to be more effective than the free Imatinib.

Once again the cytotoxic effect of Imatinib will have to be tested at a broader concentration range of the drug to accurately determine the IC_{50} values. Upon obtaining these IC-50 values combinations of the two drugs will be tested against NB cell lines to see if synergism might be present. Based on preliminary findings by our collaborator, Dr. Timeus, and a previous study our lab published on Neuroblastoma [25] that shows protective benefits of the rHDL nanoparticles against normal tissues; we believe that the rHDL formulations of these drugs will enhance their combinatorial effects *in-vitro* [2], and allow for further advancement of this novel treatment option toward the clinic.

REFERENCES:

[1] Hanahan and Weinberg. Hallmarks of Cancer: The Next Generation. *Cell.* 2011; 144: 646-674.

[1] John M Maris, Michael D Hogarty, Rochelle Bagatell, Susan L Cohn. Neuroblastoma. *Lancet.* 2007; 369: 2106–20.

[2] Timeus, et al. *In vitro* anti-neuroblastoma activity of saquinavir and its association with imatinib. *Oncology Reports*. 2012; 27(3): 734-740.

[3] Lucas Moreno, MD, PhD, Sucheta J. Vaidya, MD, C. Ross Pinkerton, MD, Ian J. Lewis, MD, John Imeson, MSc, David Machin, PhD, and Andrew D. J. Pearson, MD on behalf of the European Neuroblastoma Study Group and the Children's Cancer and Leukaemia Group (CCLG) (formerly UKCCSG). Long-Term Follow-Up of Children With High-Risk Neuroblastoma: The ENSG5 Trial Experience. *Pediatric Blood Cancer*. 2013; 60:1135–1140.

[4] Thomas Perwein, MD,* Herwig Lackner, MD, Petra Sovinz, MD, Martin Benesch, MD, Sandrin Schmidt, MD, Wolfgang Schwinger, MD, and Christian Urban, MD. Survival and Late Effects in Children With Stage 4 Neuroblastoma. *Pediatric Blood Cancer.* 2011; 57:629–635.

[5] AA Takwi, Y-M Wang, J Wu, M Michaelis, J Cinatl and T Chen. miR-137 regulates the constitutive androstane receptor and modulates doxorubicin sensitivity in parental and doxorubicin-resistant neuroblastoma cells. Oncogene 2013; 1 – 13.

[6] Frances J Sherom. ABC multidrug transporters: structure, function and role in chemoresistance. Pharmacogenomics. 2008; 9(1): 105-127.

[7] Tasnim Ara, Rie Nakata, Michael A. Sheard, et al. Critical Role of STAT3 in IL-6-Mediated Drug Resistance in Human Neuroblastoma. *Cancer Research.* 2013; 73(13); 3852–64.

[8] Shuang Yan, Zhijie Li and Carol J Thiele. Inhibition of STAT3 with orally active JAK inhibitor, AZD1480,
decreases tumor growth in Neuroblastoma and Pediatric Sarcomas *In vitro* and *In vivo. Oncotarget.*2004; 4: 433-445.

[9] Chung-Pu Wu, Chia-Hung Hsieh and Yu-Shan Wu. The Emergence of Drug Transporter-Mediated Multidrug Resistance to Cancer Chemotherapy. *Molecular Pharmaceutics.* 2011; 8: 1996-2011.

[10] Cheng-Jun Chen, Jian-Cheng Wang*, En-Yu Zhao, Ling-Yan Gao, Qiang Feng, Xiao-Yan Liu,
Zhi-Xia Zhao, Xiao-Fei Ma, Wen-Jie Hou, Liang-Ren Zhang, Wan-Liang Lu, Qiang Zhang. Self-assembly cationic nanoparticles based on cholesterol-grafted bioreducible poly(amidoamine) for siRNA delivery. *Biomaterials.*2013; 1-14.

[11] B. Ozpolat, A. K. Sood & G. Lopez-Berestein. Nanomedicine based approaches for the delivery of siRNA in cancer. *International Journal of Internal Medicine.* 2009; 267: 44-53.

[12] Shahzad, McConathy WJ, Prokai L, Lacko AG, Sood, et all. Targeted delivery of small interfering RNA using reconstituted high density lipoprotein nanoparticles. *Neoplasia*. 2011;13(4): 309-319.

[13] J.L. Markman, et al., Nanomedicine therapeutic approaches to overcome cancer drug resistance, *Advanced Drug Delivery Review.* 2013; http://dx.doi.org/10.1016/j.addr.2013.09.019

[14] Lígia C. Gomes-Da-Silva, Nuno A. Fonseca, Vera Moura, Maria C. Pederoso De Lima, Sérgio Simões, AND João N. Moriera. Lipid-Based Nanoparticles for siRNA Delivery in Cancer Therapy: Paradigms and Challenges. *Accounts of Chemical Research.* 2012; 45(7): 1163-1171.

[15] Lacko AG, Nair M, Paranjape S, Johnson S, McConathy WJ. High density lipoprotein complexes as delivery vehicles for anticancer drugs. *Anticancer Research*. 2002; 22: 2045–2049.

[16] Lacko AG, Nair M, Paranjape S, Mooberry L, McConathy WJ. Trojan horse meets magic bullet to spawn a novel, highly effective drug delivery model. *Chemotherapy*. 2006; 52(4):171–173.

[17] McConathy WJ, Nair M, Paranjape S, Mooberry L, Lacko AG. Evaluation of synthetic/reconstituted high density lipoproteins (rHDL) as delivery vehicles for paclitaxel. *Anticancer Drugs*. 2008;19(2):183–188.

[18] Kiichiro Beppu, Jerry Jaboine, Melinda S. Merchant, Crystal L. Mackall, Carol J. Thiele. Effect of Imatinib Mesylate on Neuroblastoma Tumorigenesis and Vascular Endothelial Growth Factor Expression. *Journal of the National Cancer Institute.* 2004; 96(1): 46-55.

[19] Frank Pajonk, Judith Himmelsbach, Katrin Riess, et al. Saquinavir Inhibits Proteasome Function and Causes The Human Immunodeficiency Virus (HIV)-1 Protease Inhibitor Apoptosis and Radiosensitization in Non-HIV-associated Human Cancer Cells. *Cancer Research.* 2002; 62:5230-5235.

[20] Karen McLean, Natalie A. VanDeVen, Dorothy R. Sorenson, Sayeema Daudi, J. Rebecca Liu. The HIV protease inhibitor saquinavir induces endoplasmic reticulum stress, autophagy, and apoptosis in ovarian cancer cells. *Gynecologic Oncology.* 2009; 112:623-630.

[21] Takayuki Ikezoe, Eric S. Daar, Jun-ichi Hisatake, Hirokuni Taguchi and H. Phillip Koeffler. HIV-1 protease inhibitors decrease proliferation and induce differentiation of human myelocytic leukemia cells. *Blood.* 2000; 96(10): 3553-3559.

[22] Elena Toschi, Cecilia Sgadari, Laura Malavasi, Ilaria Bacigalupo, Chiara Chiozzini, Davide Carlei,
Daniela Compagnoni, Stefania Bellino, Roberto Bugarini, Mario Falchi, Clelia Palladino, Patrizia Leone,
Giovanni Barillari, Paolo Monini and Barbara Ensoli. Human immunodeficiency virus protease inhibitors reduce the growth of human tumors via a proteasome-independent block of angiogenesis and matrix metalloproteinases. *Internation Journal of Cancer.* 2011; 128: 82-93.

[23] Kazufumi Honda, Masaya Ono, Miki Shitashige, Mari Masuda, Masahiro Kamita, Nami Miura and Tesshi Yamada. Proteomic Approaches to the Discovery of Cancer Biomarkers for Early Detection and Personalized Medicine. *Japanese Journal of Clinical Oncology.* 2013; 43(2): 103–109.

[24] Yoshiyuki Suehara, Tadashi Kondo, Kunihiko Seki, et al. Pfetin as a Prognostic Biomarker of Gastrointestinal Stromal Tumors Revealed by Proteomics. *Clinical Cancer Research.* 2008; 14:1707-1717.

[25] Nirupama Sabnis, Suraj Pratap, Irina Akopova, PaulW. Bowman and Andras G. Lacko. Pre-clinical evaluation of rHDL encapsulated retinoids for the treatment of neuroblastoma. *Frontiers in Pediatrics.* 2013; 1: 1-10.